Macromolecular Bioscience
www.mbs-journal.de



# Biocompatible Polymer-Modified Nanoplatform for Ferroptosis-Enhanced Combination Cancer Therapy

*Meng He, Yuxin Dan, Mingsheng Chen, and Chang-Ming Dong**

**Ferroptosis is a novel type of iron-dependent non-apoptotic pathway that regulates cell death and shows unique mechanisms including causing lipid peroxide accumulation, sensitizing drug-resistant cancers, priming immunity by immunogenic cell death, and cooperatively acting with other anticancer modalities for eradicating aggressive malignancies and tumor relapse. Recently, there has been a great deal of effort to design and develop anticancer biocompatible polymeric nanoplatforms including polypeptide and PEGylated ones to achieve effective ferroptosis therapy (FT) and synergistic combination therapies including chemotherapy (CT), photodynamic therapy (PDT), sonodynamic therapy (SDT), photothermal therapy (PTT), gas therapy (GT) including nitric oxide (NO), carbon monoxide (CO), and hydrogen sulfide ($H_2S$), and immunotherapy (IT). To be noted, the combo therapies such as FT-CT, FT-PTT, FT-GT, and FT-IT are attracting much efforts to fight against intractable and metastatic tumors as they can generate synergistic antitumor effects and immunogenic cell death (ICD) effects or modulate immunosuppressive tumor microenvironments to initiate strong antitumor immunity and memory effects. The polymeric Fenton nano-agents with good biosafety and high anticancer efficacy will provide a guarantee for their applications. In this review, various biocompatible polymer-modified nanoplatforms designed for FT and combo treatments are summarized for anticancer therapies and discussed for potential clinical transitions.**

## 1. Introduction

Cancer remains a dominant cause of death worldwide and will continue to be a kind of intractable disease threatening human life and health.[1] Unfortunately, due to the heterogeneity of tumors and the lack of treatment specificity, conventional cancer treatments including surgery, radiotherapy (RT), and chemotherapy (CT) often cause various side effects, a high risk of recurrence and metastasis, and a decrease in immunity.[2,3] Therefore, it is urgently necessary to develop more precise and effective therapies to combat cancer. In those cases, polymeric nanoparticles have bright prospects for more selective cancer treatments due to their adjustable physicochemical properties and unique metabolic pathways in vivo, and they are prone to accumulate at the tumor lesions due to the abnormal vasculature and dysfunctional lymphatic drainage within the tumor microenvironment (TME).[4] More importantly, the optimal drug-loading or conjugated nanoparticles can be used to integrate different drugs for programmed release of drugs in response to physiological or external stimuli under TME to reduce adverse effects for combination and cocktail chemotherapies.

Over the past two decades, extensive efforts have been devoted to develop polymeric nanoparticles serving as multifunctional diagnostic and therapeutic nanoplatforms, and some of them have been used in the clinic or trials.[5] To further enhance the therapeutic efficacy and reduce side effects, some minimally invasive treatment methods based on nanoparticles have been developed, such as photothermal therapy (PTT),[6] photodynamic therapy (PDT),[7] sonodynamic therapy (SDT),[8] starvation therapy,[9] and so on, providing new avenues for effective cancer therapies. However, the organ and cell/subcellular targeting, antitumor efficacy, and especially clinical translation of those nanoplatforms are far from satisfactory. Therefore, developing innovative therapeutic modalities are still necessary beside a deeper understanding of the interactions of biological systems and nanoparticles.

Considering that cancer cells are more susceptible to oxidative damage than normal cells, stimuli can be introduced to boost oxidative stress to disrupt the redox balance for anticancer therapy. Over the past decade, ferroptosis has been intensively studied as an iron-dependent non-apoptotic programmed cell death mode as proposed by Stockwell and colleagues in 2012.[10] Ferroptosis is characterized by the accumulation of reactive oxygen species (ROS) and lipid peroxides (LPO) to lethal levels.[10] Due to its non-apoptotic and unique cell-killing nature, ferroptosis is expected to bypass the shortcomings of traditional therapies mediated by the apoptotic pathway.[11–13] Remarkably,

M. He, Y. Dan, C.-M. Dong
School of Chemistry and Chemical Engineering
Frontiers Science Center for Transformative Molecules
Shanghai Key Laboratory of Electrical Insulation and Thermal Aging
Shanghai Jiao Tong University
Shanghai 200240, P. R. China
E-mail: cmdong@sjtu.edu.cn
M. Chen
Shanghai Public Health Clinic Center
Fudan University
Shanghai 201508, P. R. China

The ORCID identification number(s) for the author(s) of this article can be found under https://doi.org/10.1002/mabi.202300215

**DOI: 10.1002/mabi.202300215**

 

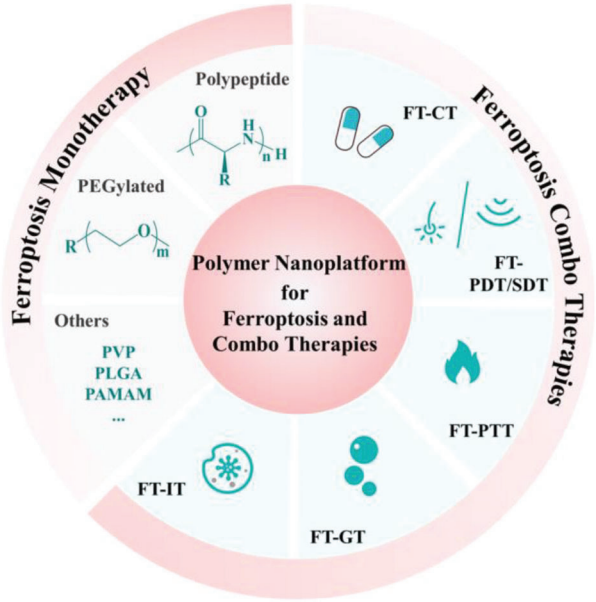


**Scheme 1.** Schematic illustration of polymer nanoplatform for ferroptosis (including polypeptide, PEGylated, and others) and combo therapies, including chemotherapy (CT), photo/sonodynamic therapy (PDT/SDT), photothermal therapy (PTT), gas therapy (GT), and immunotherapy (IT).

ferroptosis has also been involved in cancer immunotherapy to enhance potential applications.[14,15] For those purposes, biocompatible polymeric nanomaterials have been utilized to achieve ferroptosis therapies, which have hydrophilic segments for improved biodegradability and biocompatibility, thereby prolonging blood circulation to improve pharmacokinetics and therapeutic effects.[16,17]

To the best knowledge of ourselves, there are few reviews on the recent applications of biocompatible polymer nanomaterials in ferroptosis therapy (FT) and its combo therapies. Therefore, it is necessary to elucidate the rationale of constructing biocompatible polymeric nanomaterials to activate ferroptosis, introduce the latest development of ferroptosis, and summarize the combo therapies of ferroptosis with conventional or emerging therapies, including CT, PDT/SDT, PTT, gas therapy (GT), and immunotherapy (IT), as illustrated in **Scheme 1**. Finally, the limitations and the perspectives will be briefly discussed. We believe that biocompatible polymer nanomaterials in cancer ferroptosis treatments will open up a unique avenue for fighting against cancers, holding great potentials for the clinical applications.

## 2. Anticancer Applications of Ferroptosis

Ferroptosis is a ROS-dependent form of cell death associated with two main biochemical features, iron accumulation and lipid peroxidation.[12] The classical ferroptosis activator erastin or RSL3 increases intracellular iron accumulation to inhibit the antioxidant system.[18,19] Iron can directly generate excess ROS through the Fenton reaction, resulting in increased oxidative damage. In addition, iron can increase the activity of some enzymes responsible for lipid peroxidation and oxygen homeostasis.[12] Increased iron uptake or decreased iron output will make cancer cells sensitive to oxidative damage and ferroptosis, during which excess ROS would cause lipid peroxidation, protein oxidation, and DNA oxidative damage, resulting in tumor cell death.[10,13,20] Moreover, to meet rapid proliferation, cancer cells have a higher demand for iron than normal cells, which also opens up the possibility of targeting ferroptosis.[21,22] Collectively, the iron-mediated Fenton chemistry to generate excess ROS is an important pathway for iron-induced ferroptosis, and various biocompatible polymer nanomaterials have been developed for ferroptosis-based cancer therapy.

### 2.1. Biocompatible Polymer Nanoplatform for Ferroptosis Monotherapy

The biocompatibility and biosafety of Fenton nano-catalysts play a key role in guaranteeing their further clinical translation. Commonly used biocompatible polymers include but are not limited to polypeptide, polyethylene glycol (PEG), poly(vinylpyrrolidone) (PVP), polyethyleneimine (PEI), poly(lactic-co-glycolic acid) (PLGA), and poly(vinyl alcohol) (PVA),[23] in which biodegradable polypeptide and biocompatible PEG have been widely investigated for anticancer therapies with some clinical products. So the following mainly focuses on three sections on polypeptide, PEG, and other biocompatible polymers-modified nanomaterials for cancer ferroptosis.

#### *2.1.1. Polypeptide-Containing Nanomaterials*

Among numerous polymers, polypeptides possess rich side-chain functionalities, diverse hydrophilicity/hydrophobicity profiles, and stable secondary structures in solution which contribute to the self-assembling characters.[24,25] The polypeptides also exhibit the following distinction, facile chemical modification, good storage stability, and ease of combination with other strategies.[16,25] Due to the diverse biomedical functions of polypeptides, it is promising to introduce polypeptides into antitumor ferrioptosis nanomaterials.

For designing of ferroptosis nano-inducers, a direct method is to incorporate small molecule ferroptosis inducers into nanovehicles. Compared with free inducers, the nanoplatforms enable improved solubility and biocompatibility, as well as increased tumor accumulation by either active or passive targeting.[26] Resistance to the occurrence of multiple drug resistance (MDR) and the formation of metastasis is conducive to improving the efficacy of tumor therapy. Due to intrinsic high MDR activity, traditional apoptotic inducers are insufficient to kill the persistent cancer cells (PCCs). However, ferroptosis shows high efficiency to eliminate cells via manipulating intracellular redox homeostasis at the EMT state. Gao et al. synthesized a type of responsive polymer micelles to aim for efficient PCCs reduction and MDR reversal by loading RSL3 (a typical ferroptosis inducer).[27] In brief, the polymer micelles were formed by self-assembly of amphiphilic methoxyl poly(ethylene glycol)-poly(L-lysine) (PEG-PLys) in an aqueous solution. PEG was selected as the hydrophilic block and polypeptide was used as multivalent hydrophobic backbone, where high hydrophobicity arachidonic acid (AA) was picked up as the side chains because it contained multiple double bonds for the ease of peroxidation-triggered cargo release (**Figure 1**A). In addition, AA as a key precursor of

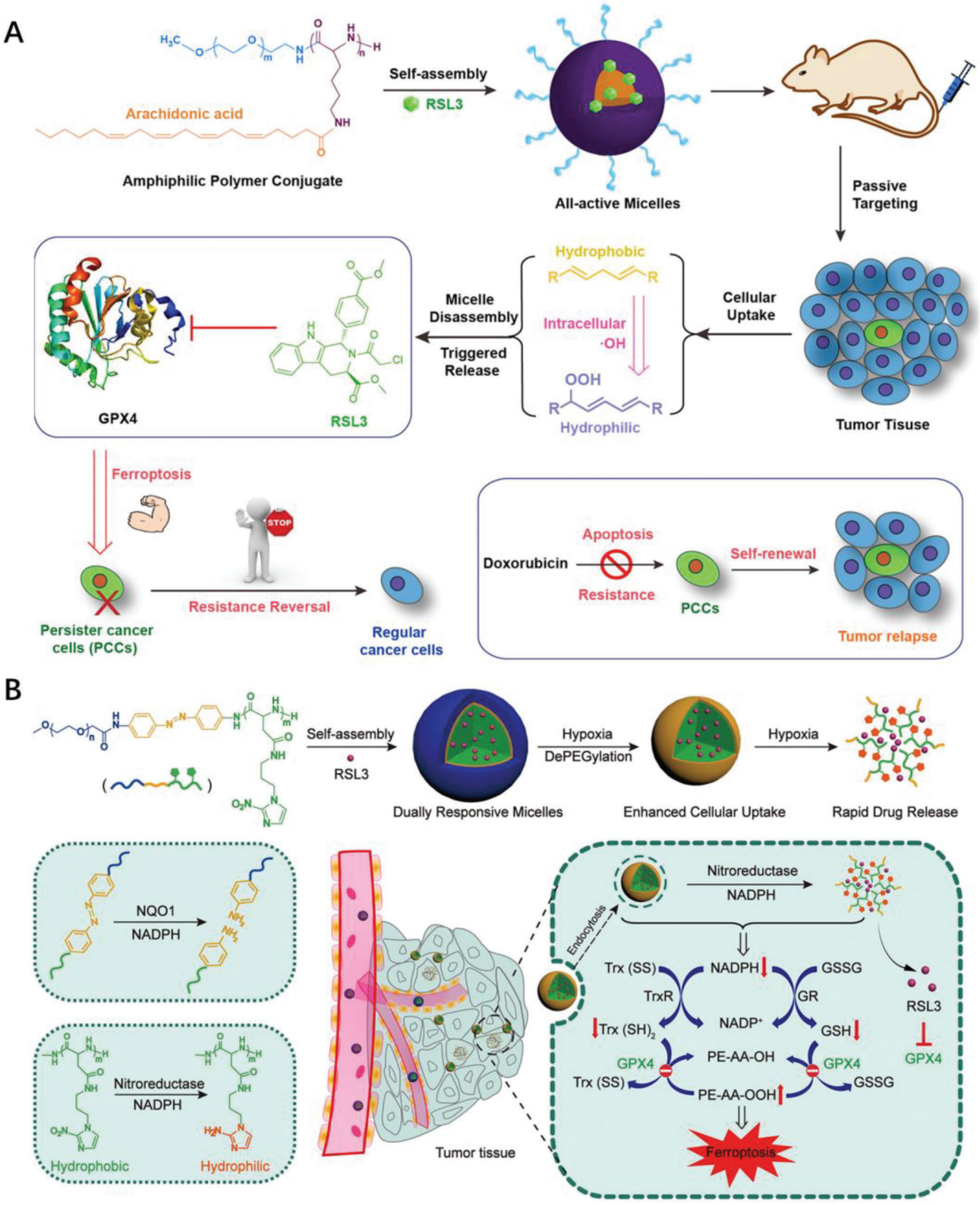


**Figure 1.** A) Schematic illustration of reactive oxygen species (ROS)-responsive polymer micelles for triggered delivery of RSL3, a model ferroptosis inducer. Reproduced with permission.[27] Copyright 2019, Elsevier. B) Schematic illustration of responsive micelles-induced NADPH depletion, glutathione (GSH), and thioredoxin diminishment and ferroptosis boosting under hypoxia. Reproduced with permission.[28] Copyright 2020, American Chemical Society.

ferroptosis not only helped to induce ferroptosis, but also played a synergistic role with the release of RSL3 in TME to effectively reduce PCCs and MDR reversal. The PEGylated polypeptide micelles showed long systemic circulation in tumor-bearing mice, benefiting their accumulation in tumors to exert therapeutic effects. And the effective elimination of PCCs through ferroptosis was achieved among the anti-doxorubicin-resistant human ovarian adenocarcinoma (DOX NAR cells) and NAR tumor-bearing nude mice. This strategy provides a potential therapeutic modality for treating MDR tumors and preventing tumor recurrence. To enhance the antitumor effect of ferroptosis under hypoxic conditions, Guo et al. designed a hypoxia-responsive polymer micelle with the purpose of reducing glutathione and thioredoxin (Figure 1B).[28] The hydrophilic PEG segment was linked with the nitroimidazole-conjugated polypeptide through an azobenzene, and the designed polymers self-assembled into nano-micelles to solubilize hydrophobic RSL3. Interestingly, the azobenzene moieties made PEG shed under hypoxia to enhance cellular uptake, while the nitroimidazole moieties were reduced by the overexpressed nitroreductase, leading to diminish intracellular glutathione and thioredoxin and enhance ferroptosis in solid tumor. In vivo efficacy of ferroptosis via depleting glutathione and thioredoxin was demonstrated in a 4T1 tumor xenograft mouse model.

Besides incorporating small molecule ferroptosis inducers into nanovehicles, the research also focuses on nanomaterials themselves which can induce ferroptosis by participating in biochemical reactions and interfering the metabolic balance. Nanomaterials can prime ferroptosis by regulating iron and ROS metabolism, and excess ROS can be generated from various sources to trigger the well-known LPO accumulation. In view of this, Wang et al. have constructed a multifunctional polymeric nanoparticles, which were co-assembled by the diblock copolymers containing PEG and poly(glutamic acid) modified by $\beta$-cyclodextrin ($\beta$-CD), ferrocene (Fc) carboxylic- acid hexadecyl ester, and ascorbyl palmitate. The PEG shells and host-guest interactions between $\beta$-CD and Fc moieties improved the stability of micelles in a serum-containing medium. What's more, the ascorbic acid at pharmacological concentration promoted the production of $H_2O_2$ in tumors, and the Fc groups further catalyzed a fast production of ·OH to prime FT.

#### 2.1.2. Biocompatible PEGylated Nanomaterials

Polymeric PEGylation is one widely-used approach to fabricate stealthy nanoparticles in research and clinical fields, and there are lots of PEGylated nanomaterials being investigated for anticancer ferroptosis applications. For instance, Kim et al. reported the nanoparticle ferroptosis inducer in 2016, in which $\alpha$MSH-PEG-C' dots were composed of near-infrared (NIR) fluorescent ultrasmall silica as C' dots, coated with PEG to form PEGylated C' dots, and then surface-modified with $\alpha$-melanocyte-stimulating hormone ($\alpha$-MSH) as a targeting ligand (**Figure 2**A).[29] Note that the precursor nanoparticle of C' dots, known as Cornell dots, had received FDA New Drug approval. Incubation of the $\alpha$MSH-PEG-C' dots with tumor cell lines under amino acid starvation conditions triggered effective ferroptosis. Mechanistically, the C' dots with deprotonated surfaces could recruit iron from the extracellular environment, and their fractal internal structure and high surface-to-volume ratio were also beneficial for iron absorption. Therefore, the PEGylated C' dots entry into cancer cells could highly increase intracellular iron content and induce massive ROS production and GSH depletion, eventually leading to heavy ferroptosis (Figure 2B). In vivo experiments confirmed $\alpha$MSH-PEG-C' dot played an effective ferroptosis in multiple cancer models (Figure 2C–E).

A more direct method is to construct the iron-containing nanoparticles that can deliver and release iron ions into cancer cells. Iron-based nanomaterials such as superparamagnetic iron oxide nanoparticles, iron nanometallic glasses, iron cross-linked gel nanoparticles, iron-containing metal–organic frameworks, and mesoporous silica nanomaterials (MSN) have been extensively tested as ferroptosis agents. For instance, Wang et al. reported on the iron engineering of MSN into $rFeO_x$-HMSN nanocatalyst with intrinsically catalytic functionality and stimuli-responsive biodegradability.[30] PEG/$rFeO_x$-HMSN could convert abundant $H_2O_2$ in tumor into hydroxyl radicals in TME and induce severe oxidative stress, including lipid peroxidation and further mitochondrial/DNA damage, achieving an efficient tumor suppression. Importantly, the 4T1 tumor growth was effectively suppressed by the intratumor or intravenous injection of PEG/rFeOx-HMSN.

#### 2.1.3. Other Biocompatible Polymer-Modified Nanoparticles

Although PEG is commonly considered safe, increasing evidence has shown that repeating injections of PEG-protein conjugates and PEGylated nanodrugs would elicit immunological responses including hypersensitivity and so-called accelerated blood clearance effect.[24] From this point of view, more robust methods are necessary to synthesize other alternative biocompatible polymers. To date, a variety of hydrophilic polymers including but not limited to polypeptide -, -PVP-, polyglycerol, zwitterionic polymers (e.g., polybetaines), poly(2-oxazoline)s, and glycopolymers have been investigated as possible alternatives to PEG for different biomedical applications.[23] Meanwhile, dendritic polymers including commercially available polyamide-amine (PAMAM) dendrimers have unique topology to assume multivalent functionalities in anticancer nanomedicines. To fight against pancreatic cancer, one of the most aggressive and lethal malignancies, Ma et al. proposed a generation 5 -PAMAM dendrimer-Fe(III) complex to tackle pancreatic carcinoma through apoptosis-enhanced ferroptosis therapy.[31]

Very recently, the biocompatible PVP-coated nanozyme was discovered as a tumor-specific activated therapeutic agent for dual-modality imaging-guided combination tumor therapy. Chen's group developed an activatable nanozyme-mediated 2,2′-azino-bis (3-ethylbenzothiazoline-6-sulfonic acid) (ABTS) loaded ABTS@MIL-100/PVP (AMP) nanoreactors (NRs).[32] In vivo studies revealed that the fabricated theranostics AMPNRs could be specifically activated in TME to switch on their photoacoustic imaging (PAI) and PTT functions through a nanozyme-mediated "two-step rocket launch-like" process (**Figure 3**A). Notably, the PAI signal intensity dramatically increased with time even in small tumors with volume at nearly 20 $mm^3$. Ex vivo fluorescence imaging of 4T1-tumor-bearing mice treated with Cy5@AMP was further conducted to investigate the biodistribution, and the Fe

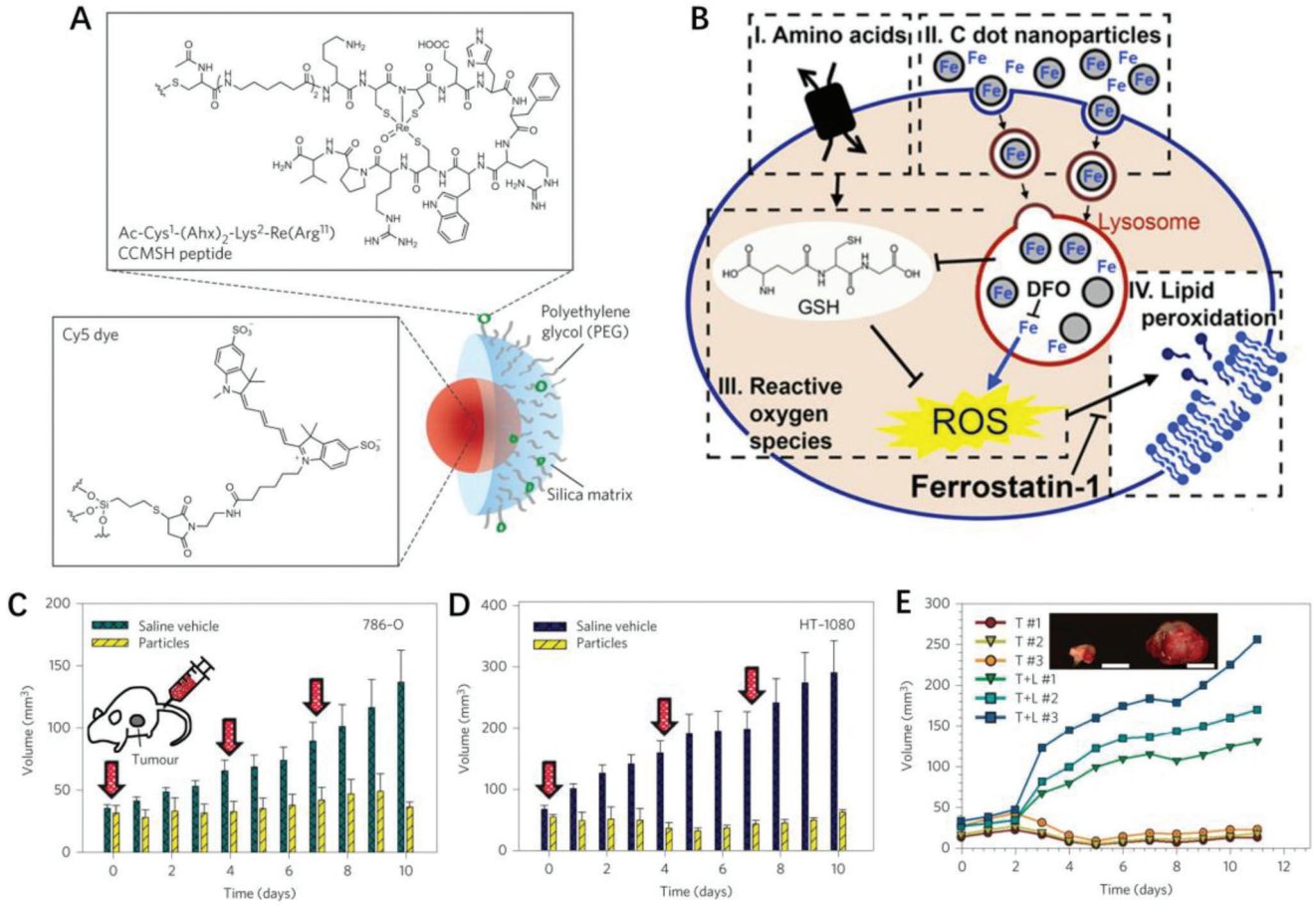


**Figure 2.** A) Structure of $\alpha$-MSH-PEG-C′ dots, where a Cy5 fluorophore is encapsulated by silica and modified with PEG, functionalized with melanoma-targeting peptide. B) Schematic illustration of the mechanism of C′ dots-induced ferroptosis. C) 786-O renal carcinoma and D) HT-1080 fibrosarcoma xenograft tumors can be suppressed by i.v. injected $\alpha$-MSH-PEG-C′ dots (particles, 12 nmol × 3 dose, $n = 5$). E) Volume variation of individual HT-1080 xenograft tumor in mice after different treatments. Reproduced with permission.[29] Copyright 2016, Springer Nature.

content in the tumors was as high as ≈4.67% of the injected dose per gram tissue (%ID $g^{-1}$) at 24 h post-injection, confirming a good tumor accumulation (Figure 3B,C). In vivo complete suppression of tumor growth and no further recurrence were found during the period of treatment (Figure 3D–F), being attributed to the simultaneous production of ·OH and scavenging GSH. In all, this nanozyme-mediated nanoreactor could be used for dual-modal imaging-guided and TME-triggered PTT-FT, demonstrating effective therapeutic efficacy with minimal side effects.

Collectively, the biocompatible polymer-modified iron-containing nanomaterials have presented unique cancer cell-killing mechanism via the non-apoptotic LPO accumulation pathway, which is induced by the well-known intracellular Fenton reaction and is mainly dependent on the iron concentration and $H_2O_2$ content in tumors. Despite versatile strategies that have been conceived to deliver high concentrated irons into tumor cells while the lower $H_2O_2$ content still limits the kinetics of the Fenton reaction, the resultant ·OH concentration and the ferroptosis efficacy. So the combo ferroptosis therapies based on biocompatible polymer-modified nanomaterials that can enhance antitumor FT efficacy via synergistic effect will be discussed in the following section.

### 2.2. Biocompatible Polymer Nanoplatform for FT-Involved Combination Therapies

The heterogeneity of cancer determines that antitumor monotherapy cannot treat various cancer cell subpopulations with different genotypes and phenotypes.[22] Although many biocompatible therapeutic FT nanoplatforms have been developed, the FT monotherapy often fails to eradicate cancer cells, leading to tumor recurrence and metastasis. In recent years, FT has shifted from improving the Fenton/Fenton-like catalytic effect of FT agents to combo therapies, such as -CT-, PTT, PDT, and SDT. In many cases, the combo therapy is not just a simple addition, but generate synergistic anti-tumor effect of "1+1 > 2-" or even "1+1+1 > 3-", boosting antitumor efficacy for potential clinical applications.

#### *2.2.1. Combo FT-CT*

Up till now, CT is still one of the most widely used for cancer treatments in clinics besides surgery. However, CT has its limitations that including unsatisfactory efficacy, potential cytotoxicity, and

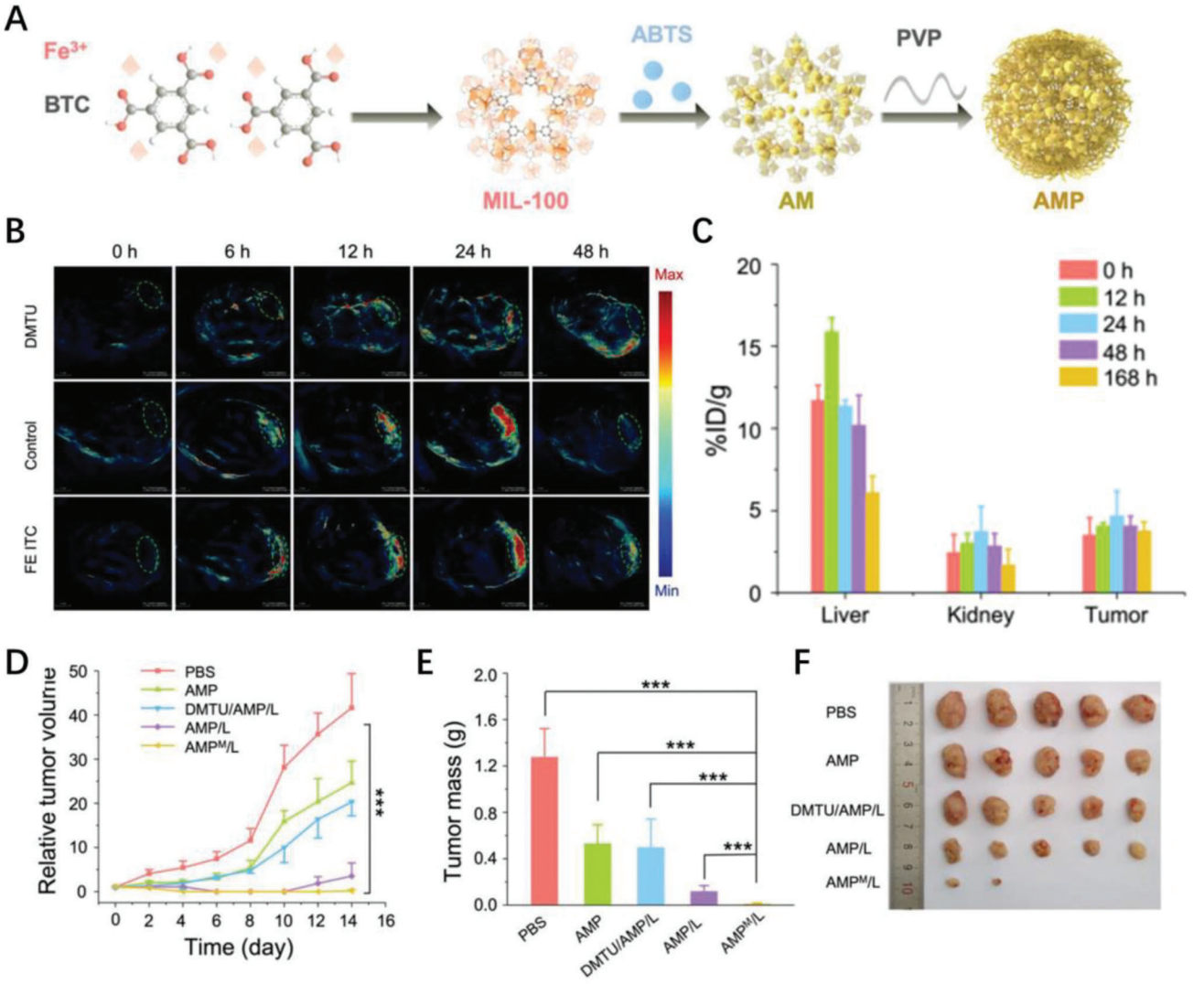


**Figure 3.** A) Preparation procedure of AMP NRs. B) Representative PAI images of tumor with different treatments as a function of post-injection time of AMP NRs. C) Biodistribution of AMP NRs in liver, kidney, and tumor. The amount of Fe in different samples was analyzed by ICP-AES. D) The relative tumor volume of 4T1-tumor-bearing mice treated with different formulations as a function of time. E) The average tumor mass and F) photo of excised tumors of different groups on the 14th day. Reproduced with permission.[32] Copyright 2019, Wiley-VCH.

narrow treatment window.[33] When loaded in the nanoparticle delivery systems, those drugs have an improvement in delivery efficiency and therapeutic efficacy. Recently, some strategies for combining CT and FT have been proposed including platinum-based drugs and doxorubicin (DOX) which have been frequently applied in clinical CT. For example, cisplatin can be utilized to generate superoxide radical ($O_2^{\cdot -}$) and its downstream molecules of $H_2O_2$, and then produce ROS via the Fenton reaction.[34] Ma et al. reported a sequential drug delivery strategy based on the intracellular release of iron ions from iron oxide nanoparticle to sensitize cisplatin.[35] With an iron oxide nanoparticle coated by -(PEI- and PEG, FePt-NP2 was constructed after loading cisplatin prodrugs (**Figure 4**). FePt-NP2 could guide MRI imaging and deliver iron to the tumors, while the cisplatin prodrugs were reduced into toxic cisplatin to form Pt-DNA adducts, thus causing tumor apoptosis. On the other hand, the released cisplatin activated nicotinamide adenine dinucleotide phosphate (NADPH) oxidase (NOX) to trigger $O_2$ to produce abundant $O_2^{\cdot -}$, which was subsequently converted to $H_2O_2$ by superoxide dismutase (SOD). Since FePt-NP could be hydrolyzed in cells to self-sacrifice and release a high content of active iron ions, and $H_2O_2$ was further catalyzed to form excessive highly toxic ·OH, leading to fast oxidation of lipids and proteins and DNA damage. This work specifically exploits both DNA targeting and ROS-producing capabilities of a toxic cisplatin drug, which subsequently activated the iron-dependent Fenton reaction to enhance the synergistic efficacy of FT-CT. Moreover, the peptide-based therapeutic carriers are also promising for platinum-based drug delivery. Gao et al. encapsulated iron oxide nanoparticles and anticancer Pt prodrug into a polypeptide nanocarrier through an electrostatic self-assembly process, for $T_2$-weighed MRI and FT-CT combo therapy.[36] The number of iron oxide per polypeptide nanocarrier

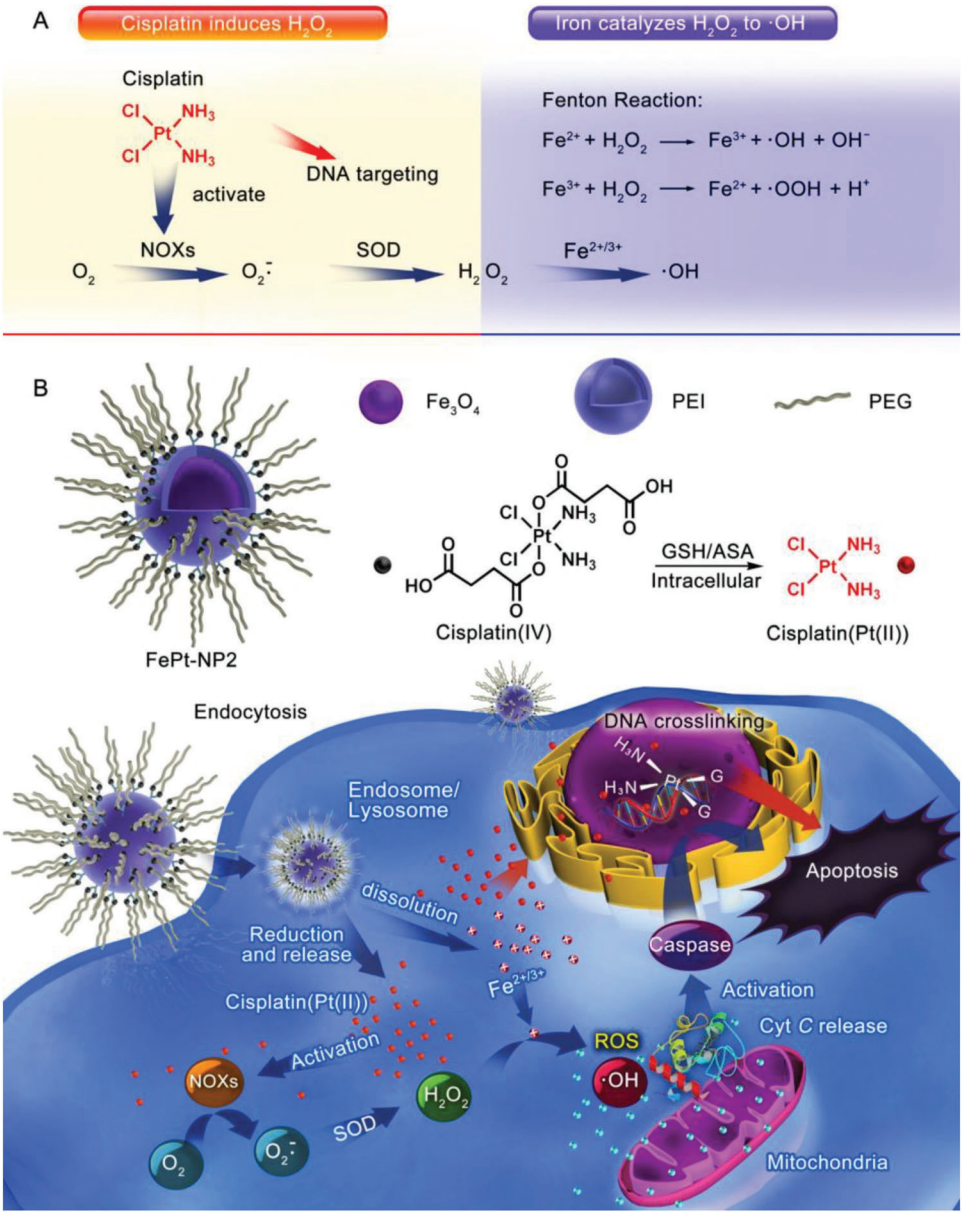


**Figure 4.** Maximizing cisplatin efficacy by constructing self-sacrificing iron-oxide nanoparticles with cisplatin (IV) drugs FePt-NP2 for synergistic actions. A) Cisplatin activates NOX, catalyzes the formation of superoxide and $H_2O_2$ from $O_2$, and iron catalyzes the Fenton chemistry to turn $H_2O_2$ into highly toxic ·OH. B) Construction of self-sacrificing iron oxide nanoparticles with cisplatin (IV) prodrug (FePt-NP2) circumvents the endocytosis of cisplatin into the cells, and excess ·OH cause fast lipid and protein oxidation and DNA damage, as well as apoptosis via the ROS/Cyt *C*/caspase-3 pathway. Reproduced with permission.[35] Copyright 2017, American Chemical Society.

could be controlled by adjusting initial added amount, and both Pt prodrug and iron ions were released simultaneously, triggering cascade reactions to generate ·OH for FT. The released Pt prodrug could enter the nucleus and interact with DNA to induce apoptosis, and in vivo treatment in U87 MG tumor-bearing mice exhibited heavy tumor suppression effect.

DOX is another commonly-used drug to inhibit topoisomerase II and causes cell apoptosis,[37] and some biocompatible polymeric nanoparticles have combined DOX-based CT with FT. Jiang et al. designed a polymeric nanoparticle of P-B-D NPs that could continuously inhibit the energy metabolism of tumor cells to improve the tumor sensitivity.[38] The polymer chains were composed of PEG, disulfide bond (S-S), PEI and 1,2-distearoyl-sn-glycero-3-phosphoethanolamine (DSPE), and PEG-SS-PEI-DSPE, DOX-duplex, and a glucose transporter 1 inhibitor of BAY-876 co-assembled into a sandwiched P-B-D NPs. The disulfide bond in P-B-D NPs was cleaved by intracellular glutathione to cause collapse, and the depletion of GSH led to the inactivation of GPX4 to enhance FT. Especially, DOX-duplex could deplete ATP and release DOX to kill tumor cells, while the released BAY-876 inhibited the function of Glut1 to restrict the energy metabolism of tumor cells, and more than 90% of tumor cells were killed by

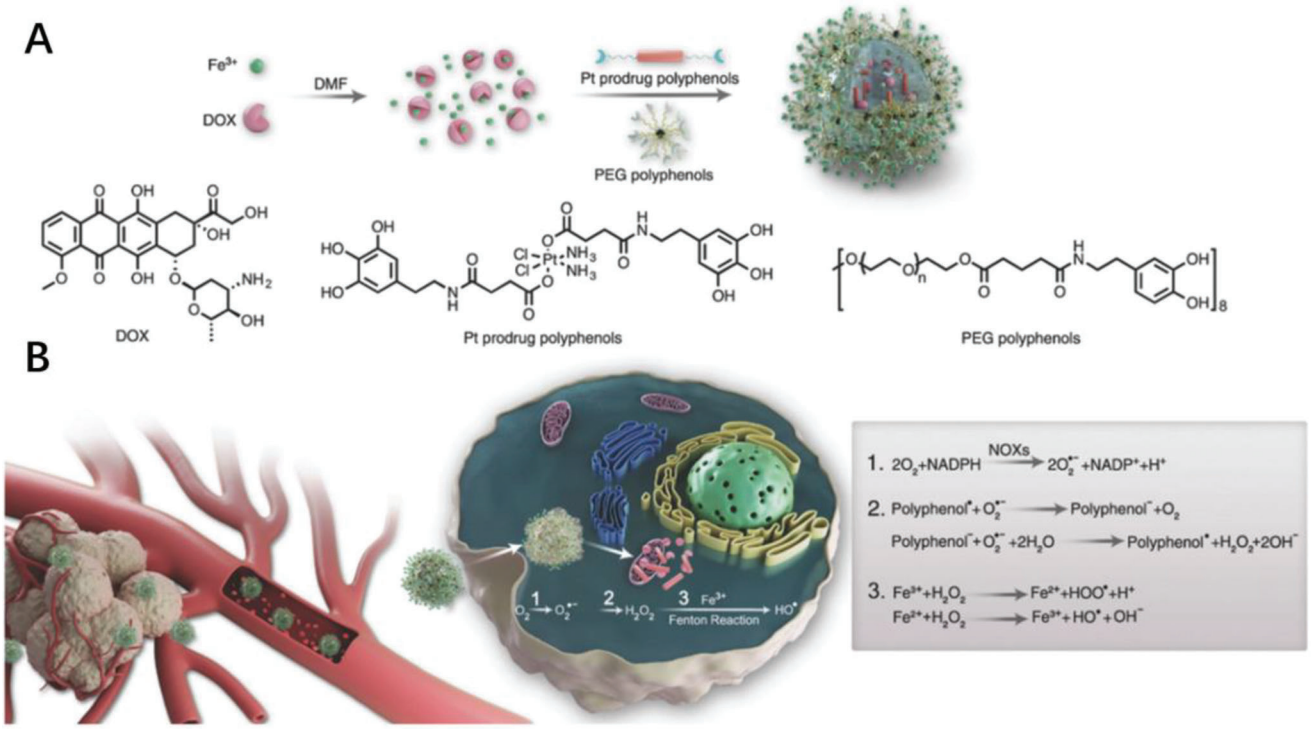


**Figure 5.** Formulation of nanoparticles and the ROS enhanced chemotherapy mechanism. A) Schematic of the DPPF NPs self-assembly process. B) The DPPF NPs accumulated in the tumor by the EPR effect and internalized in the tumor cells. Reproduced with permission.[42] Copyright 2018, Wiley-VCH.

combo FT-CT. The independent pathway between platinum drug and DOX can achieve synergistic therapeutic effect, and reduce drug resistance and side effects.[39] Moreover, both platinum drug and DOX could activate the -NADPH- oxidases to catalyze the NADPH and $O_2$ into $NADP^+$ and superoxide radical of $O_2^{\cdot-}$.[40,41] Then $O_2^{\cdot-}$ undergoes disproportionation reactions to generate $H_2O_2$ and $O_2$ to promote the Fenton/Fenton-like reaction. Dai et al. designed a ROS-enhanced nanoplatform with DOX and Pt prodrugs being encapsulated by the self-assembly of biocompatible metal-polyphenol networks.[42] $Fe^{3+}$ was coordinated with DOX, and then assembled with platinum prodrug and PEG polyphenols to form DOX@Pt prodrug Fe nanoparticles (DPPF NPs) (**Figure 5**). $Fe^{3+}$ not only served as inorganic cross-linking agent for polyphenol coordination, but also could convert $H_2O_2$ into highly toxic ·OH through the Fenton reaction to enhance CT efficacy. The combined nanoplatform improved the cocktail CT efficacy of DOX and Pt, providing a cocktail CT-PT strategy for synergistically enhancing cancer efficacy. Overall, combo FT-CT cooperatively produces optimal therapeutic efficacy via different mechanisms, in which ferroptosis can kill drug-resistant cells while the drugs can promote the ferroptosis efficacy by boosting ROS levels or others.[43]

### *2.2.2. Combo FT-SDT/PDT*

Minimally invasive _PDT- and -SDT- have received widespread attention in recent years, in which most of sound or lasers-based therapies relies on the reaction of photosensitizers or sonosensitizers. PDT utilizes lasers to activate photosensitizers (e.g., Ce6) to produce highly active singlet oxygen ($^1O_2$) via energy transfer to kill tumor cells,[44] while SDT exerts an antitumor effect by ultrasound-activated sonosensitizers (e.g., protoporphyrin) in tumors.[45] The common character of PDT, SDT, and FT is that they are all based on ROS-mediated cancer therapies, while the difference is that PDT and SDT produce singlet oxygen, but FT mainly produces hydroxyl radicals of ·OH.[46,47] Despite different reaction processes, they all produce highly active ROS, subsequently triggering cell death, and also promoting ferroptosis by disrupting redox homeostasis via the GSH consumption to inactivate GPX4 indirectly and sensitize tumor cells.[47,48] Therefore, the polymeric nano-systems for the co-delivery of photosensitizers or sonosensitizers and ferroptosis inducers have been intensively studied for synergistic cancer therapies.[48]

On the combo FT-PDT, Chen et al. reported an integrated nanoparticle for triple-negative breast cancer treatment,[49] and they loaded Ce6 and $Fe_3O_4$ with -PLGA- to obtain $Fe_3O_4$-PLGA-Ce6. Specifically, $Fe^{3+}/Fe^{2+}$ could react with $H_2O_2$ to produce ·OH via the Fenton reaction, resulting in intracellular ROS accumulation, LPO generation and GSH depletion while singlet $^1O_2$ produced by the PDT effect of Ce6 could also induce tumor cells death to boost ferroptosis. Tumor hypoxia is a prominent phenomenon in the TME, which limits the efficacy such as PDT. To overcome the shortcoming, Zhao et al. proposed a FT-PDT strategy to regulate hypoxic TME using a ROS-activatable liposomes (RALP).[50] RALP@HOC@$Fe_3O_4$ contained egg-yolk L-$\alpha$-phosphatidylcholine- as the lipid component, a thioketal bond-linked conjugate of PEG and photosensitizer cypate- as functional segments, $Fe_3O_4$ nanoparticles as a crucial component utilizing the Fenton reaction and oxaliplatin prodrug for smart

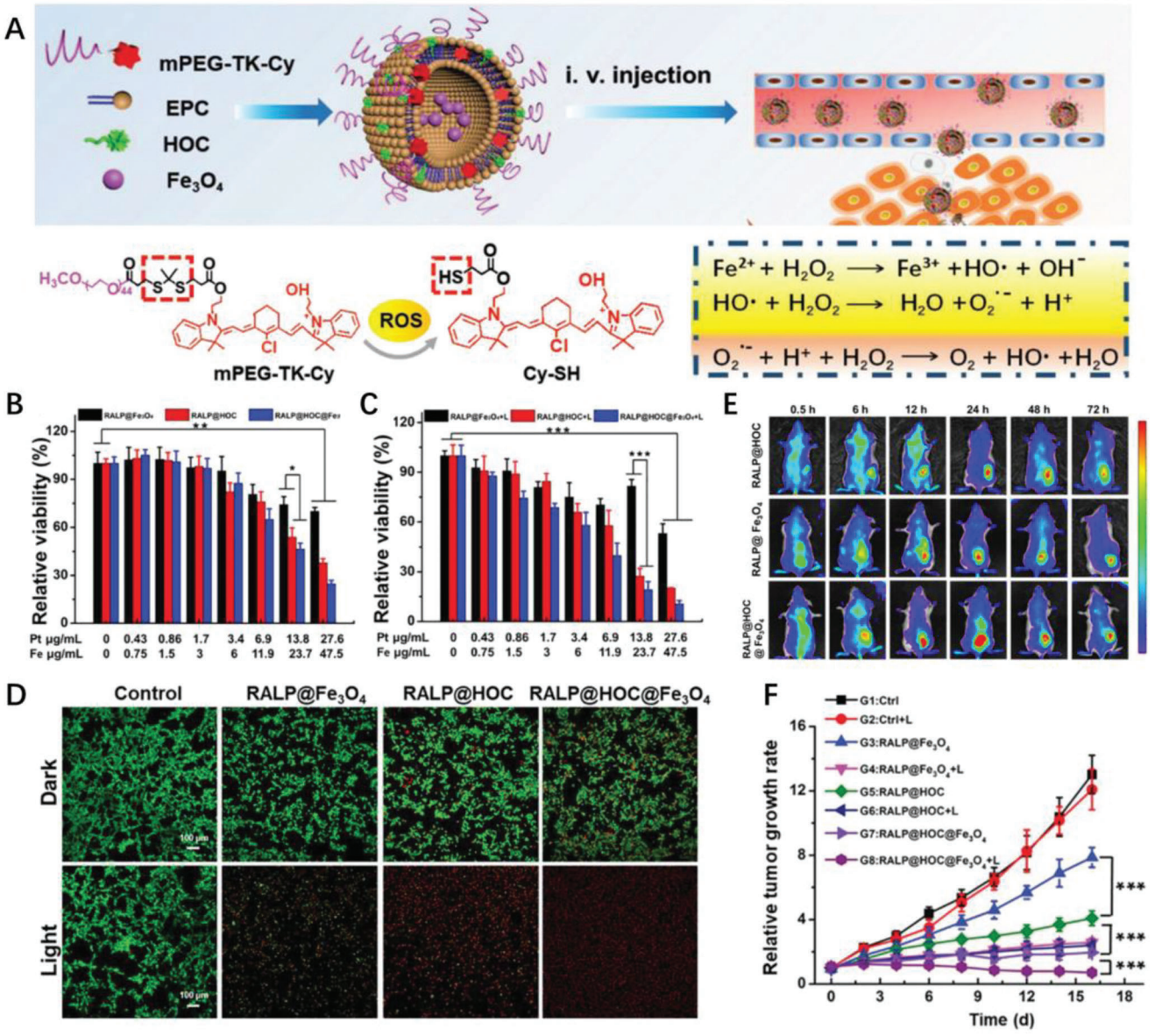


**Figure 6.** A) Synthesis of RALP@HOC@$Fe_3O_4$ and drug administration in vivo (i.v. injection). Cytotoxicity of RALP@HOC@Fe3O4, RALP@HOC, and RALP@Fe3O4 against CT-26 cells B) in the dark and C) with 808 nm laser irradiation (1.0 W $cm^{-2}$, 5 min). D) Fluorescence images of CT-26 cells in live-dead staining experiments w/o laser irradiation. E) Fluorescence imaging of RALP@$Fe_3O_4$, RALP@HOC, RALP@HOC@$Fe_3O_4$ distribution in CT-26 tumor-bearing mice. F) Changes in the relative tumor volumes after different treatments ($n = 6$) (* $p < 0.05$, *** $p < 0.001$). Reproduced with permission.[50] Copyright 2019, Wiley-VCH.

regulation of hypoxia TME (**Figure 6**A). RALP@HOC@$Fe_3O_4$ could enhance photosensitization and exert cytotoxic ROS-mediated effect (Figure 6B,C), which especially overcame the tumor hypoxia in PDT and the lower efficacy in FT because oxaliplation prodrug reacted with GSH to break the delicate redox equilibrium in tumor cells. Besides, in vivo assessments suggested that RALP@HOC@$Fe_3O_4$ induced synergistic ROS generation, and improved tumor oxygenation in CT-26 tumor-bearing mice (Figure 6D–F).

Due to the strong penetrating ability of ultrasound in tissues, SDT can achieve effective therapy for deep tumors.[51] Based on ROS-producing nanodrugs combining SDT with FT, Li et al. designed amphiphilic PEG-polylysine copolymers linking with a mechanophore of Fc-,[52] and they self-assembled into a model sonosensitizer of protoporphyrin IX encapsulated micelles (**Figure 7**A). During ultrasound treatment, $^1O_2$ and ·OH were produced to induce apoptosis via combo SDT-FT. Meanwhile, the ROS-induced GSH consumption boosted ferroptosis that were promoted by the conversion of Fc to $Fe^{2+}$ by $H_2O_2$ in TME. Moreover, Fc-triggered dissociation also activated the release of sonosensitizer (PpIX), overcoming short half-life and limited diffusion distance of therapeutic ROS. The induction and sensitization interplay between apoptosis and ferroptosis was further substantiated in a 4T1 tumor-bearing mice model

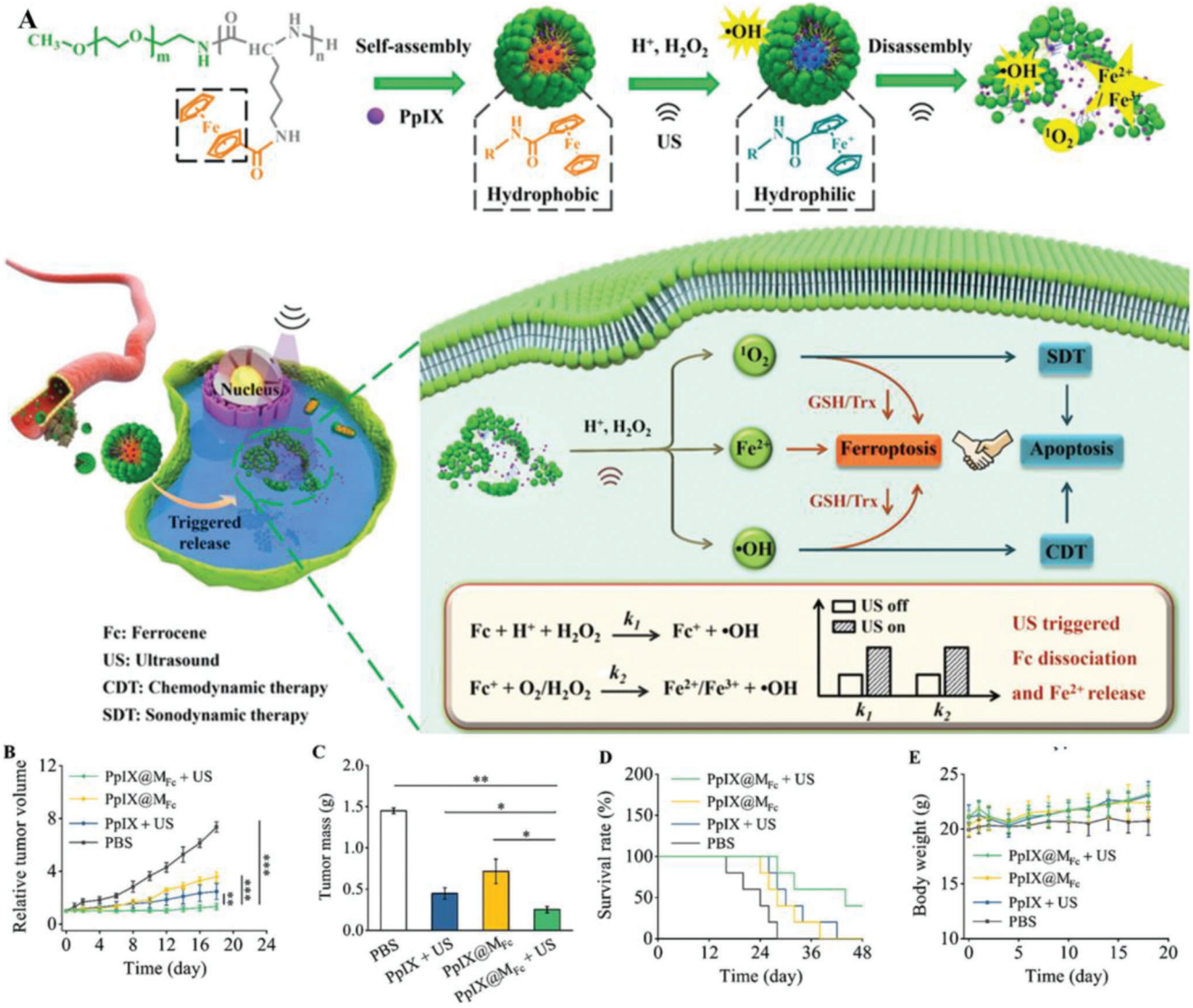


**Figure 7.** A) Schematic illustration of the mechano-responsive micelles (PpIX@MFc) for apoptotic and ferroptotic cancer therapy. The -Fc-bearing amphiphilic polymer- self-assemble into micelles wherein the model drug PpIX is loaded. B) Tumor growth inhibition curve. C) The average weight of solid tumor groups on the 18th day. D) Kaplan–Meier mice survival curve of mice. E) Kinetic mice body weight during the therapeutic period. Reproduced with permission.[52] Copyright 2022, Wiley-VCH.

(Figure 7B–E). Meanwhile, Bai et al. synthesized ultrasmall iron-doped titanium dioxide nanodots (Fe-$TiO_2$ NDs) by thermal decomposition strategy, which were stabilized by PEG modification for dual-modal imaging-guided SDT-FT synergistic therapy.[53] To alleviate the adverse effects of abnormal tumor blood vessels and dense extracellular matrix and improve the efficacy of SDT, Lin and co-authors prepared ≈20 nm Au-MnO Janus NPs (JNPs) with ultrasound and GSH dual-responsivity to realize SDT-FT.[54] Such JNPs were coated with hydrophilic thiolated PEG-SH and hydrophobic ROS-sensitive poly(1,4-phenyleneacetone dimethylene thioketal) (PPADT-SH) to yield JNP@PEG/PPADT vesicles. Under ultrasound stimulation, these vesicles dissociated into small Janus Au-MnO nanoparticles, and then into smaller Au nanoparticles, improving the permeability. At the same time, the generation of ROS was enhanced, thereby improving the efficiency of SDT. Obviously, the exogenous ROS generated by nano-photo/sonosensitizers during PDT or SDT leads to severe LPO accumulation and ferroptosis, thus combo FT-PDT/SDT might bypass the apoptotic pathway and thereby overcome intrinsic resistance to apoptosis in some tumors, while this is largely unexplored and deserves to be deeply investigated in ongoing work.

### 2.2.3. Combo FT-PTT

Tumor tissue is more sensitive to heat than normal one and can be irreversibly damaged once the temperature exceeds 43 °C.[55] PTT agents can convert near-infrared light into thermal energy, thus PTT is spatiotemporally controllable, possessing the characteristics of minimal invasiveness and high selectivity.[56]

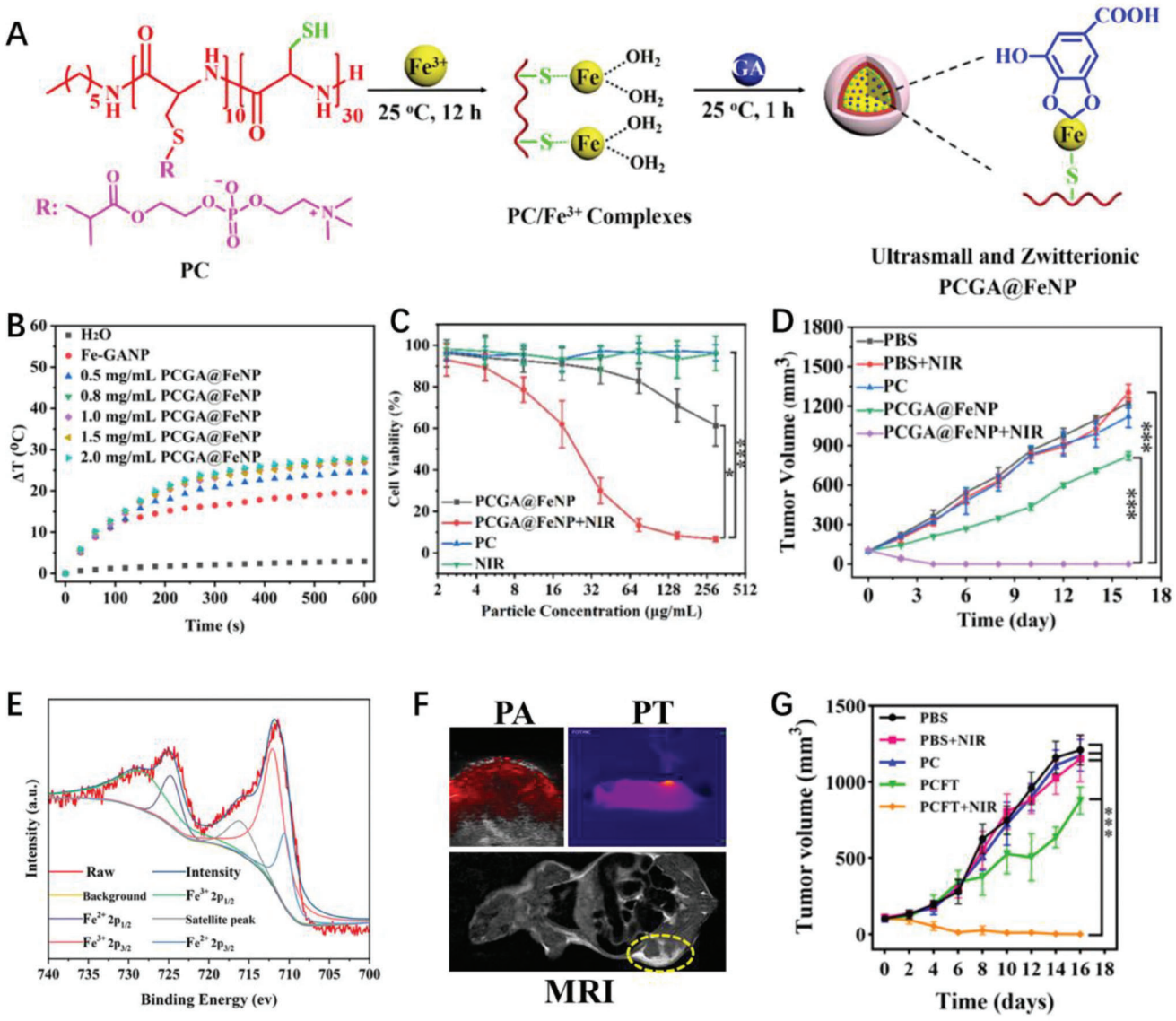


**Figure 8.** A) Fabrication of Ultrasmall Zwitterionic Polypeptide Coordination Nanohybrids of PCGA@FeNP. B) the NIR-mediated temperature elevation of PCGA@FeNP prepared at different PC concentrations. C) Cytotoxicity of PCGA@Fe-NPs incubated with 4T1 cells with/without NIR irradiation (808 nm, 1 W $cm^{-2}$, 10 min; $n = 6$, $*p < 0.05$, $***p < 0.001$). Reproduced with permission.[61] Copyright 2021, American Chemical Society. D) Tumors' change. E) XPS of PCFT. F) In vivo PCFT-mediated trimodal imaging of PAI, PTI, and MRI in 4T1 tumor-bearing mice ($n = 4$). G) Tumor volume dependent on the post-injection time. Reproduced with permission.[62] Copyright 2022, American Chemical Society.

Imaginably, PTT can ablate the tumor in situ and accelerate the Fenton reaction to achieve combo FT-PTT, causing a synergistic effect to enhance anticancer efficacy. To achieve effective tumor ablation, a high temperature of above 50 °C is usually required for PTT monotherapy.[57] Liu et al. explored a nanomotors (PHPF NMs) with hemin and-Fc - depositing on the surface of bowl-shaped polydopamine (PDA) for PTT and FT.[58] Owing to the superior photothermal conversion capacity of PDA, PHPF NMs could rapidly elevate the tumor temperature by ≈20 °C within 10 min of 808 nm laser irradiation (1.6 W $cm^{-2}$). The photothermia could accelerate the release of hemin and -Fc from PHPF NMs, which further reacted with endogenous $H_2O_2$ to increase ·OH generation and consumed GSH for the FT-PTT. However, a high temperature of above 50 °C would cause severe damage to normal tissues. Therefore, developing mild PTT (< 50 °C) coupled FT is urgent as it preferentially eliminates tumors without causing considerable damage to normal tissues or inducing inflammation.[59,60]

Aiming for highly efficient combo FT with mild PTT, Dong et al. have devoted to designing the polypeptide nanocomposites in recent years. They have prepared a ultrasmall zwitterionic polypeptide-coordinated nanohybrids (PCGA@FeNP) to ablate 4T1 solid tumors via joint apoptosis and ferroptosis pathways (**Figure 8**A).[61] The zwitterionic thiols-pendant polypeptide co-complexed with gallic acid (GA) and iron ions to form ultrasmall nanohybrids with ≈6 nm. Those coordinated nanohybrids

exhibited prominent photothermal conversion efficiency of ≈59.5%, unsaturated ferrous coordination, and intracellular acid responsiveness, which could accelerate the Fenton reaction to induce a synergistic effect between FT and PTT (Figure 8B). In vitro and in vivo studies demonstrated that ultrasmall PCGA@FeNP indeed mediated effective FT and FT-PTT, achieving complete and traceless 4T1 tumor ablation with a single intravenous dose and one NIR irradiation (Figure 8C,D). Furthermore, to deliver a higher concentration of iron ions for boosting FT, Dong et al. also put forward another facile strategy for constructing the iron-coordinated nanohybrid of methacryloyloxyethyl phosphorylcholine-grafted polycysteine/iron ions/tannic acid (i.e., PCFT).[62] The PCFT possessed intrinsic photothermia and the reductive iron content of ≈12.0 wt.%, which was favorable for realizing FT along with multiple imagings (Figure 8E,F), and in vivo PTT-FT treatment eradicated 4T1 tumors without skin scar and tumor recurrence for 16 days (Figure 8G). Those studies open up an avenue to overcome the poor efficacy of monotherapy FT and mild PTT via the combo mild PTT-FT treatment. However, it is not clear how to control genome reprogramming under moderate heat stress to induce tumor sensitivity to ferroptosis, as well as how to realize cell fate conversion from ferroptosis to non-ferroptotic death under external stimuli. Bearing the critical issues in mind, Xie et al. proposed a heat-triggered tumor-specific ferroptosis strategy by encapsulated $Fe_3O_4$ and 1H-perfluoropentane into PLGA-b-PEG to endow them with thermal phase transition property, and heterodimeric polypeptide on the surface of NPs was utilized as a prostate tumor-targeting agent.[63] Under NIR light-mediated moderate heat of ≈45 °C, in situ potent ROS was produced to prime FT. To be noted, it was reported that the acyl-CoA synthetase bubblegum family member 1 was an essential determinant for the ferroptosis induction in the CRPC cell line C4-2 by examining the molecular level changes in genes and the iPath pathway analysis, and moderate heat stress inhibited antioxidant pathways of tumor cells, induced reprogramming of lipid metabolism, and enhanced the therapeutic effect of ferroptosis.

The second near-infrared photothermal therapy (NIR-II PTT, 1000–1300 nm) is emerging as a new phototherapy method, which has deeper penetration, less energy dissipation, and minimal toxicity to normal tissues compared with the first NIR PTT (NIR-I PTT, 650–950 nm). However, suboptimal photothermal conversion and limited therapeutic efficacy remain major challenges for NIR-II PTT.[64] Pu et al. reported a hybrid semiconductor nanoenzyme (HSN) with photo-enhanced catalytic activity for NIR-II PAI-guided synergistic photothermal ferrotherapy.[65] The HSN backbone was an amphiphilic PEGylated semiconducting polymer, which served as both the NIR-II photothermal converter and iron chelator (**Figure 9**A). HSN was reported to have the highest photothermal conversion efficiency ($\eta$) of 98.9%, and could mediate a fast production of ·OH (Figure 9B). Excitingly, NIR-II PTT-FT could eliminate complete tumor ablation, performing better than monotherapy of NIR-II PTT or FT in vivo (Figure 9C,D). Taken together, the thermal effect generated by PTT can greatly enhance the ferroptosis effect in TME, and PTT-FT can exert a synergistic therapeutic effect to eradicate cancer. To further improve the light-to-heat conversion efficiency or tissue penetration depth, developing biodegradable polymer nanoparticles integrating combo NIR-II PTT-FT will be a meaningful direction for precise cancer treatment.

#### *2.2.4. Combo FT-GT*

-GT- is an emerging cancer treatment due to its minimal side effects, and some kinds of gases involved in physiological and pathological processes have been studied including nitric oxide (NO), carbon monoxide (CO), hydrogen sulfide ($H_2S$), and so on.[66,67] GT could kill tumor cells directly at a threshold concentration, enhancing drug accumulation in tumors, and sensitizing tumor cells to other therapies, including the combo GT-FT[67-].[67,68]

Among all harmful gas molecules, nitric oxide (NO) is widely applied in biomedical field due to its unique anti-tumor mechanisms. A high concentration of NO (>1 μM) can kill tumor cells directly through mitochondrial and DNA oxidation or nitridation, and enhance the efficacy of CT, PDT, or CDT while NO is a double-edged sword and can instead promote tumor growth at <1 μM.[69,70] For example, Zhang et al. constructed a DHA/SNP loaded nanoparticles (DHA/SNP@Zif-8) with folic acid (FA) modified PEG on its surface.[71] DHA served as a ferroptosis inducer, while SNP was the donor of $Fe^{2+}$ and NO after decomposition. The released $Fe^{2+}$ could trigger ferroptosis on one hand and NO promoted apoptosis on the other, synergistically killing tumor cells. FA is expected to bind to the highly expressed FA receptor in cancer cells for achieving tumor targeting, and DHA/SNP@Zif-8-FA gradually exhibited a better tumor suppression effect. $Fe^{2+}$ in the nanoparticles could react with DHA to enhance FT via intracellular ROS formation, and DHA and SNP synergistically played for the anti-tumor efficacy. To utilize biodegradable FDA-approved PLGA, Yang et al. designed core-shell nanoparticles of $Fe_3O_4$@PLGA/L-arginine, and combo NO-FT was capable of retarding the tumor growth in tumor-bearing mouse model.[72] Furthermore, as an endogenous signaling gas transmitter, NO has been proven effective in inhibiting cancer metastasis by regulating the expression of related proteins (e.g., MMP, E-cadherin, N-cadherin). In terms of suppressing lung metastasis of tumors, Du et al. developed D-arginine (D-Arg) internally loaded metal-organic frameworks (MOF) nanoparticles with hyaluronic acid (HA) decorated on the surface (**Figure 10**A).[73] Especially, the iron-produced ROS could react with NO derived from D-Arg to produce more toxic anions, peroxynitrite anions ($ONOO^-$), to kill tumor cells (Figure 10B–E). Even under hypoxia condition, HA@MOF/D-Arg could produce more free radicals and NO in K7M2 cells to achieve anticancer effect. Under X-ray irradiation, HA@MOF/D-Arg potently suppressed the tumor growth in mice for three weeks, thereby improving the survival rate up to 60 days and inhibiting lung metastasis simultaneously (Figure 10F,G). It is noted that NO, as a kind of reactive nitrogen species, can elevate LPO accumulation and cause ferroptosis-like cell death similar to ROS,[74] and NO can synergistically act with ferroptosis to amplify tumor immunogenic cell death and immune responses.[75]

CO in organisms is produced by heme oxygenase catalyzing the degradation of heme, and as a signal transmitter it has anti-inflammatory and cell protection effects[76] while a high concentration of CO can effectively kill cancer cells.[77] At present,

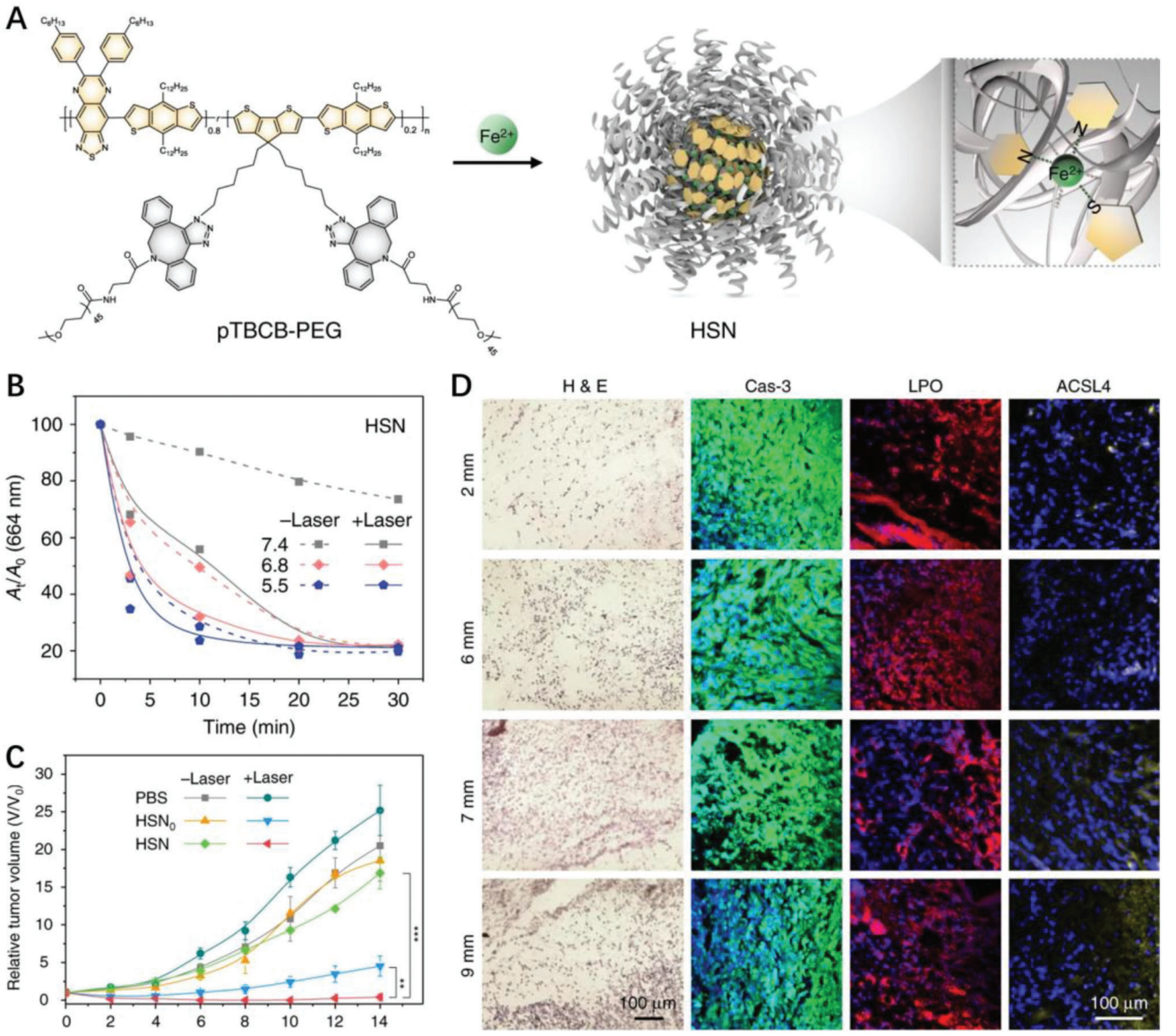


**Figure 9.** A) Chemical structure of pTBCB-PEG, preparation of HSN, and proposed mechanism of iron chelation. B) ·OH generation of HSN under different pH conditions (pH = 7.4, 6.8, 5.5) with or without 1064 nm photoirradiation (1 W $cm^{-2}$). C) Tumor growth curves of mice after photothermal ferro-therapy and monotherapies ($n$ = 3). D) H&E staining and immunofluorescent staining (Cas-3, LPO, and ACSL4) images of tumor sections at different photothermal depths after monotherapies or photothermal ferrotherapy. Reproduced with permission.[65] Copyright 2020, Springer Nature.

CO therapy mainly relies on gas donor molecules, but facing the poor solubility of donor molecules and uncontrollable potential toxicity. Aiming for CO GT-FT, Yao et al. constructed a MCN nanoplatform (FeCO-DOX@MCN) co-loaded with DOX and hydrophobic iron carbonyl (FeCO) prodrugs.[78] The released CO greatly improved the sensitivity of MCF-7 breast cancer cell line to chemotherapeutic drugs under the assistance of FT. After intravenously injected into MCF-7 tumor-bearing mice, FeCO-DOX@MCN could effectively accumulate in tumor, and 3 to 5 tumor-bearing mice in the FeCO-DOX@MCN+NIR group were completely eliminated by the combo CO-GT with CT-PTT, performing superior to single CT and/or PTT. On the other hand, -$H_2S$- can induce apoptosis and has the potential to antitumor at optimal concentrations, akin to -NO- and -CO-.[79,80] However, $H_2S$ cannot be treated by direct inhalation due to its pungent odor and toxicity. Most of the $H_2S$ donors have poor solubility and toxicity, and their effective enrichment and controlled release in tumor lesions are still clinical problems to be solved urgently.[81] The precise delivery and controlled release of $H_2S$ donors with the help of nano-platforms is a versatile way to realize $H_2S$ gas therapy for cancer. To improve the effectiveness of the ferroptosis and $H_2S$ GT, Yang et al. designed a catalysis nanoparticles by loading iron sulfide in $Fe_{1-x}S$-PVP NPs to realize the release of ·OH radicals and $H_2S$ for synergetic FT-GT (**Figure 11**A).[82] The generation of ·OH/$S^{2-}$ illustrated that $Fe_{1-x}S$ would be released and catalyzed Fenton-like reaction to produce ·OH for FT (Figure 11B,C), and subsequently some amount of $S^{2-}$ that combined with $H^+$ in the weakly acidic condition to trigger the $H_2S$

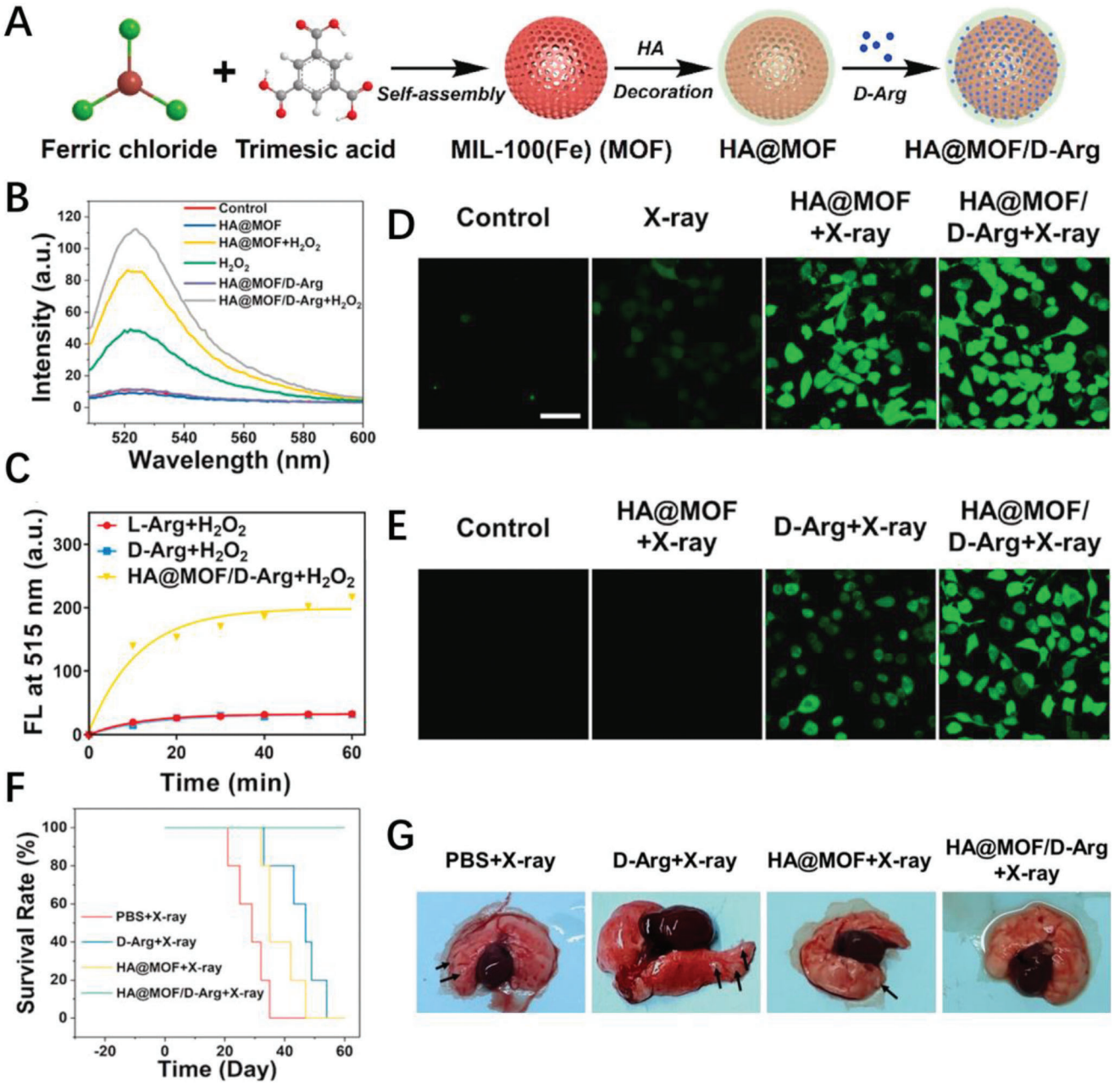


**Figure 10.** A) Schematic illustration of the synthetic route to HA@MOF/D-Arg, B) free radicals from 1 mg $mL^{-1}$ nanoparticles and/or 100 μM $H_2O_2$ were detected with the probe DCFH-DA (10 μM), C) time-course changes of the 515-nm fluorescence intensity of DAF-FM DA incubated with indicated samples, D,E) fluorescence images of K7M2 cells stained with 10 μM and 5 μM DCFH-DA upon different treatments, respectively; F) survival curves of mice after indicated treatments in 60 days, G) representative images of lungs collected from tumor-bearing mice after the survival tests. Reproduced with permission.[73] Copyright 2021, Elsevier.

production for GT. Notably, the pH sensitivity to $Fe_{1-x}S$-PVP NPs was so high that the ·OH and $H_2S$ would only release under excess $H_2O_2$ and weak acidity of pH 6.5-6.8, benefiting to enhance the efficacy (Figure 11D). In another case, a PEGylated porous molybdenum disulfide ($MoS_2$) nanoflower (MSP) as $H_2S$-transmitters was developed for FT-GT.[83] Besides having high photothermal capabilities, MSP could selectively deplete GSH through a reduction-complexation reaction, induced cellular redox dysregulation, and generated high concentrations of ROS to improve FT. The NIR irradiation-mediated PTT also promoted the $H_2S$ release and ROS production, thus $H_2S$-mediated GT and FT achieved a synergistic inhibition of MCF-7 cancer in vivo.

Considering the above-discussed NO, CO, and $H_2S$ gas therapies, the combination of FT-GT is an emerging anticancer treatment, in which NO can enhance the oxidative stress at the tumor sites to boost the LPO level for sensitizing ferroptosis.[74] Both $H_2S$ and CO can cause mitochondrial dysfunction and DNA-release, activating cyclic guanosine monophosphate-adenosine

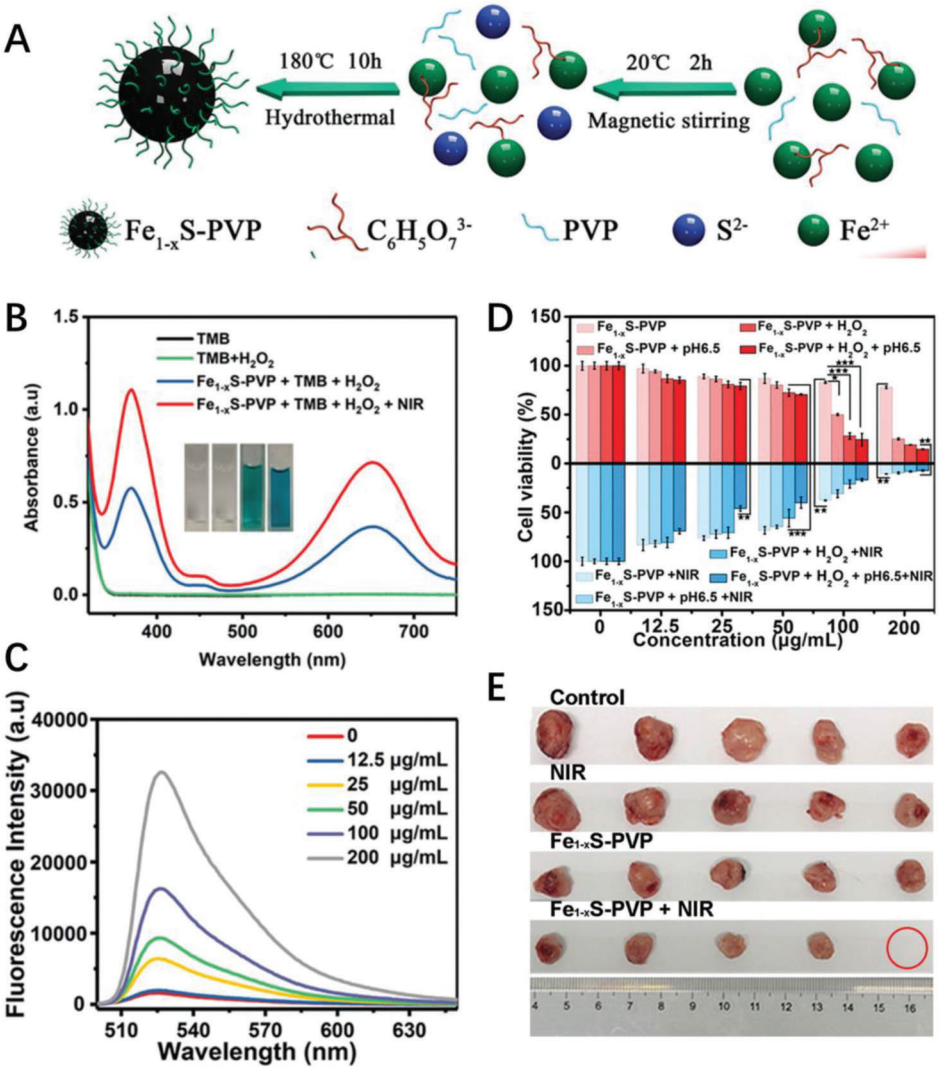


**Figure 11.** A) Schematic diagram of the Fe1−xS-PVP-mediated synergistic GT/PTT/FT treatment. B) UV–vis absorbance curve of TMB, TMB + $H_2O_2$, $Fe_{1-x}$S-PVP + TMB + $H_2O_2$, and $Fe_{1-x}$S-PVP + TMB + $H_2O_2$ + NIR. C) Fluorescence spectra of $Fe_{1-x}$S-PVP NPs in PBS (pH = 6.5) with HSip-1 at different concentrations. D) Cell viability of PAN-02 cells after therapy in different groups. E) Photograph of tumor harvested after various treatments by PBS, NIR, Fe1−xS-PVP, and Fe1−xS-PVP + NIR for 14 days. Reproduced with permission.[82] Copyright 2021, Wiley-VCH.

monophosphate synthase-stimulator of interferon genes- signaling pathway and playing as gaseous immunoadjuvants while ferroptosis can mediate tumor immunogenic cell death to prime the immunity.[84] However, the gas donor delivery still suffers from how to implement the precise and spatiotemporal delivery and dose in the tumor sites, besides the disadvantages of short half-life, lower loading efficiency, and complex carrier structures, all of which make it difficult to exert synergistic FT-GT therapy. Notably, the synergistic antitumor mechanism on combo FT-GT deserves to be further investigated in ongoing work.

### 2.2.5. Combo FT-IT

Immunotherapy harnesses the natural immune system to identify, attack, and eradicate cancer cells against tumor metastasis and recurrence.[85] Currently, innovative immunotherapies, such as immune checkpoint blockade (ICB) strategies,[86–89] cancer vaccines,[90] and chimeric antigen receptor T cell - therapy,[91,92] have achieved encouraging clinical outcomes. However, some shortcomings involving high economic cost, low immune response rate, limited antitumor efficacy, and some severe side effects hamper the progress of immunotherapies.[93,94] Fortunately, combo FT-IT provides enormous potential for the eradication of primary and metastatic tumors via a synergistic mechanism of immunogenic cell death (ICD) and/or reversal of immunosuppressive TME.[15,95,96] Song et al. designed an acidity-activatable nanoplatform BNP@R to elicit immunogenic activation by inducing ferroptosis in tumor cells.[97] The nanoparticles were composed of intracellular-acidity-ionizable PEG-b-poly(2-(diisopropylamino) ethyl methacrylate) and acid-liable phenylboronate ester dynamic covalent bonds for loading RSL-3 through hydrophobic and $\pi$–$\pi$ stacking interactions (**Figure 12**A). The nanoparticles would dissociate significantly

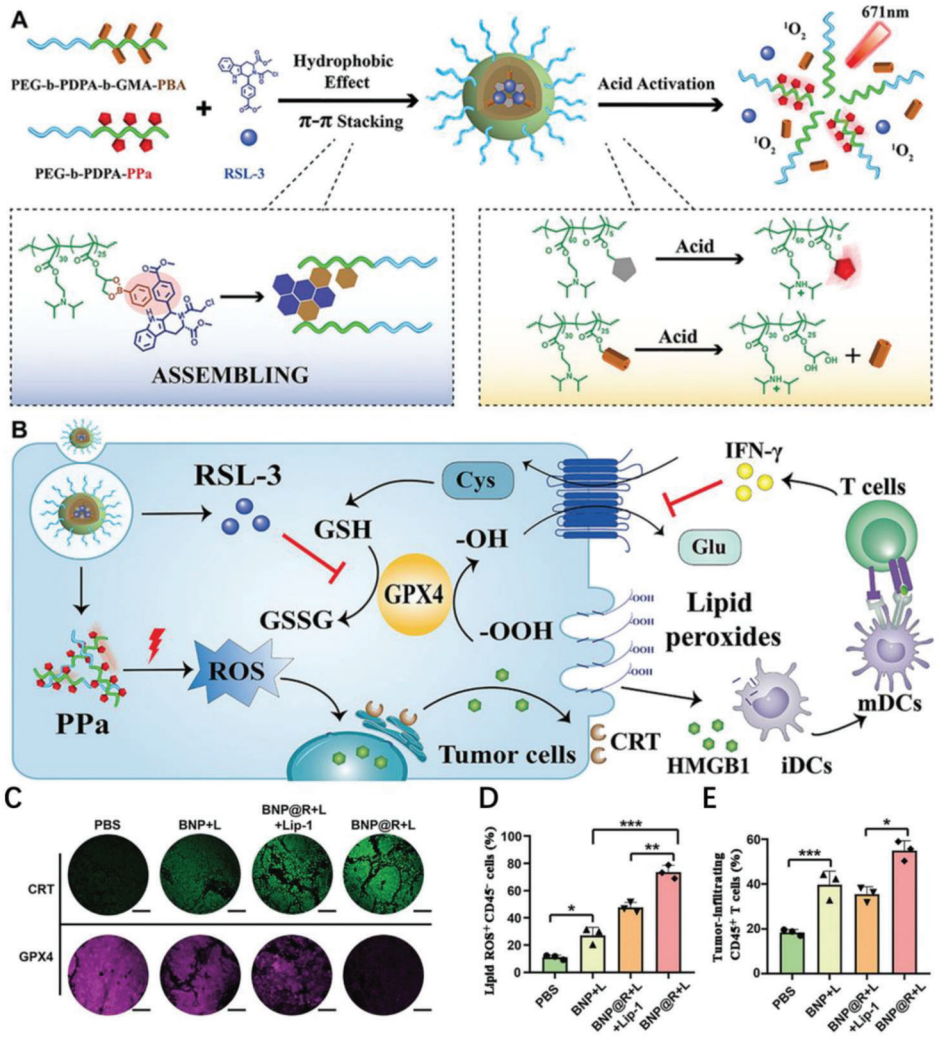


**Figure 12.** A) Fabrication of the acidity-activatable dynamic nanoparticles, B) acid-triggered RSL-3 release and activation of photoactivity of the PPa-conjugated nanoparticles, C) immunofluorescence staining of CRT and GPX4 expression in the tumor sections, and D,E) flow cytometry analysis of intracellular lipid ROS accumulation in $CD45^-$ tumor cells and treatment-induced intratumoral infiltration of $CD3^+$ - at 5 days post three cycles of treatments. Reproduced with permission.[97] Copyright 2021, Wiley-VCH.

in endocytic vesicles, triggering the release of RSL-3, initiating secretion of IFN-$\gamma$, and consequently priming tumor cells to GPX4-related ferroptosis. Tumor cells undergoing ferroptosis inhibited the expression of GPX4, promoted the expression of ICD, alleviating the immunosuppressive TME, thereby activating immunity in vivo (Figure 12B). Beside good anti-cancer effect in B16-F10 melanoma model, an excellent anti-lung metastasis effect was realized in 4T1 tumor plus anti-PD-L1 antibody, indicating that FT can improve the efficacy of cancer immunotherapy (Figure 12C–E).

Despite the application of $Fe_3O_4$ nanoparticles in cancer theranostics, however few scientists pay attention to their positive immune-stimulating functions. As one of the most aggressive cancer types, malignant melanoma is prone to local or distant metastasis, especially in the lungs. For promising clinical application, Luo et al. used ultra-small $Fe_3O_4$ NPs as nano-immunity enhancers and OVA as a model antigen to prepare $Fe_3O_4$ NPs-OVA nano-vaccine, which could effectively stimulate the maturation of BMDCs, activated T cells and macrophages, thus inhibited the growth of subcutaneous B16-OVA tumors and prevented metastasis in vivo.[98] This work provides a promising strategy for expanding potential use of Fe-based nanomaterials. Xie et al. constructed a novel phototherapeutic metal-polyphenol network to realize anti-exosomal PD-L1 synergistic ferroptosis-enhanced tumoridal immunotherapy.[99] They prepared phototheranosic metal-phenolic networks (MPNs) using PEG-modified semiconducting polymers. In this nanoplatform, $Fe^{3+}$ as a good ferroptosis inducer could effectively coordinate with the phenolic groups, and hydrophilic PEG could ensure to form stable ferrous MPNs (**Figure 13**A), and a hydrophobic exosome inhibitor-GW4869 was encapsulated to form pH-responsive PFG MPNs. PFG MPNs generated heat via PTT-induced ICD to release DAMPs for promoting DC maturation. Importantly, the GW4869 exosomal inhibitor could break the inhibition of PD-L1 to restore T cells function and secrete high levels of IFN-$\gamma$. In the resistant B16F10 bilateral tumor model, the increase in frequency of DC matura-

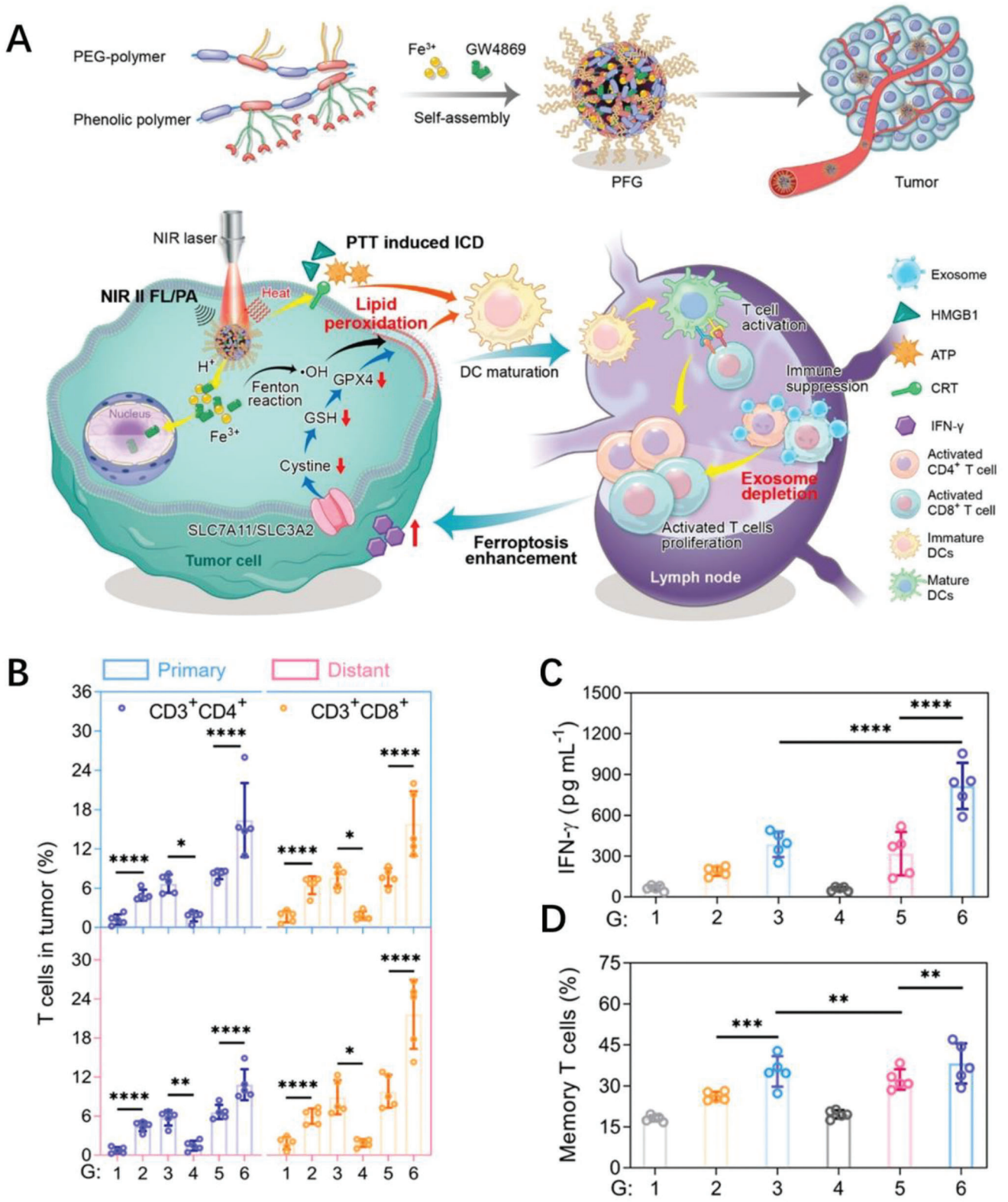


**Figure 13.** A) Schematic illustration of PFG MPNs for phototheranostic effect, relief of exosomal immunosuppression, ferroptosis enhancement, and immune stimulation. B) Representative flow cytometric quantification of intratumoral infiltration of CD4+ and CD8+ T cells (gating on CD3+ T cells). C) IFN-$\gamma$ secretion level in sera of mice. D) Flow cytometric analysis of memory T cells ($CD44^{high}CD62L^{low}$, gating on $CD3^+CD8^+$ T cells) in the spleen. Data were presented as the mean ± sd ($n = 5$). Reproduced with permission.[99] Copyright 2022, American Chemical Society.

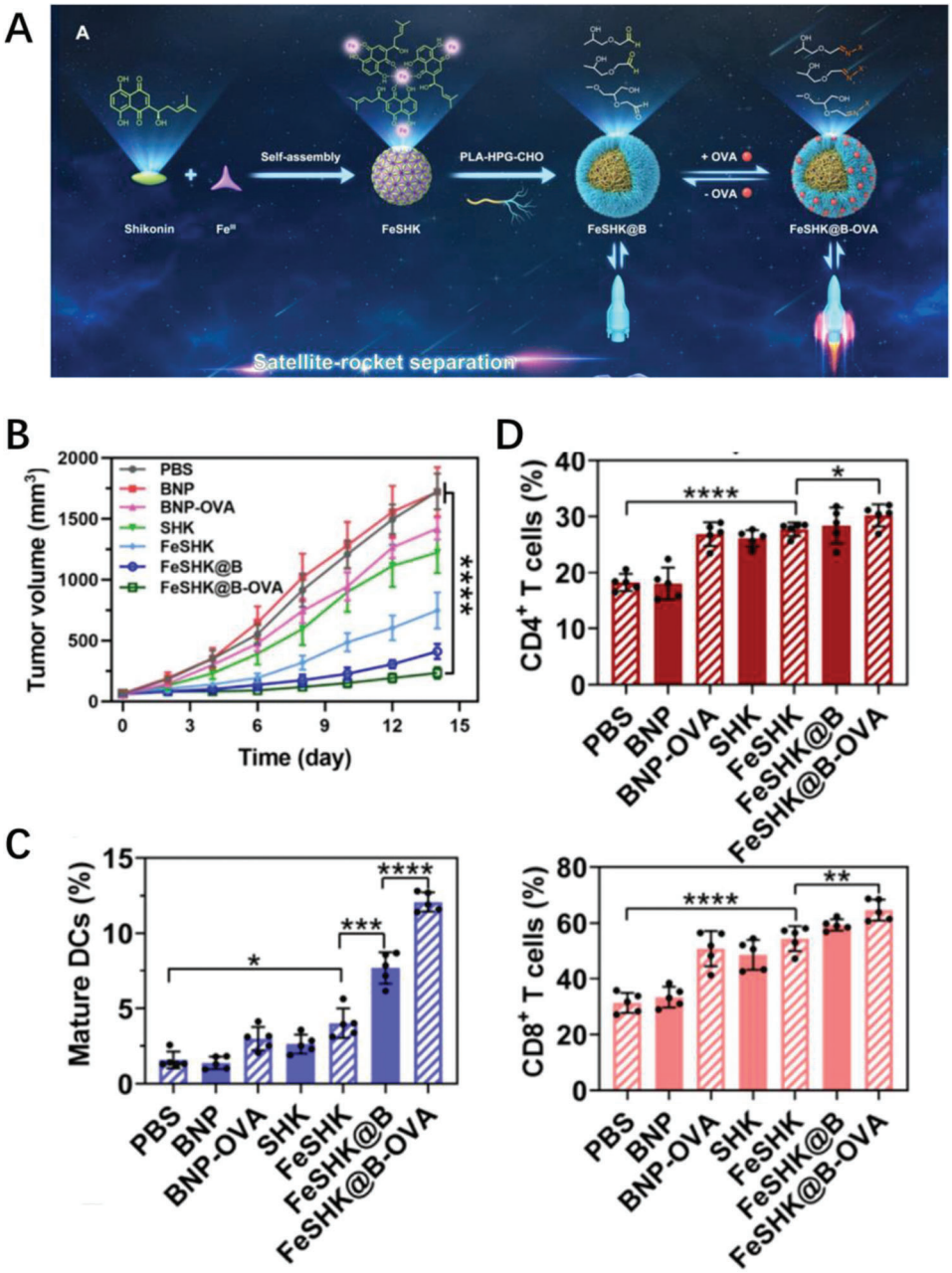


**Figure 14.** A) Synthetic procedure of the FeSHK@B-OVA "nanorocket", B) tumor growth curves of the B16-OVA tumor-bearing mice during the therapy, C) quantitative analysis of mature DCs ($CD11c^+$ $CD80^+$ $CD86^+$) in tumor draining lymph nodes, and D) quantitative analyses of the intratumoral level of infiltrated $CD4^+$ T cells ($CD3^+$ $CD4^+$) and $CD8^+$ T cells ($CD3^+$ $CD8^+$). Data are presented as the mean ± SD ($n = 5$). Reproduced with permission.[100] Copyright 2023, American Chemical Society.

tion, helper T cells, and cytotoxic T lymphocytes - in primary and distant tumors were observed owing to the photothermal immunity and the anti-exosomal PD-L1 enhanced ferroptosis, along with the variations of cytokines and the proportion of memory T cells, demonstrating that mutually reinforcing PTT-induced ICD and anti-exosomal PD-L1 enhanced ferroptosis, evoking potent antitumor immunity in B16F10 tumors and immune memory against metastatic tumors in lymph nodes (Figure 13B–D).

Due to tumor heterogeneity and immunosuppressive TME, most cancer vaccines primarily target a single antigen and TME, leading to unsatisfactory therapeutic efficacy. Recently, Yang et al. reported a bio-adhesive nanoparticle (BNP)-based cancer vaccine of FeSHK@B-OVA, which could target multiple tumor antigens and implement effective cancer immunotherapy.[100] FeSHK@B-OVA, being called as "nano-rocket", could start the "satellite rocket separation" program in acidic TME, during which the FeSHK@B "launch vehicle" continuously amplified the oxidative stress in cells and transformed primary tumors into antigen depots, and further cooperated with OVA "satellites" to trigger powerful antigen-specific antitumor immunity (**Figure 14**A).

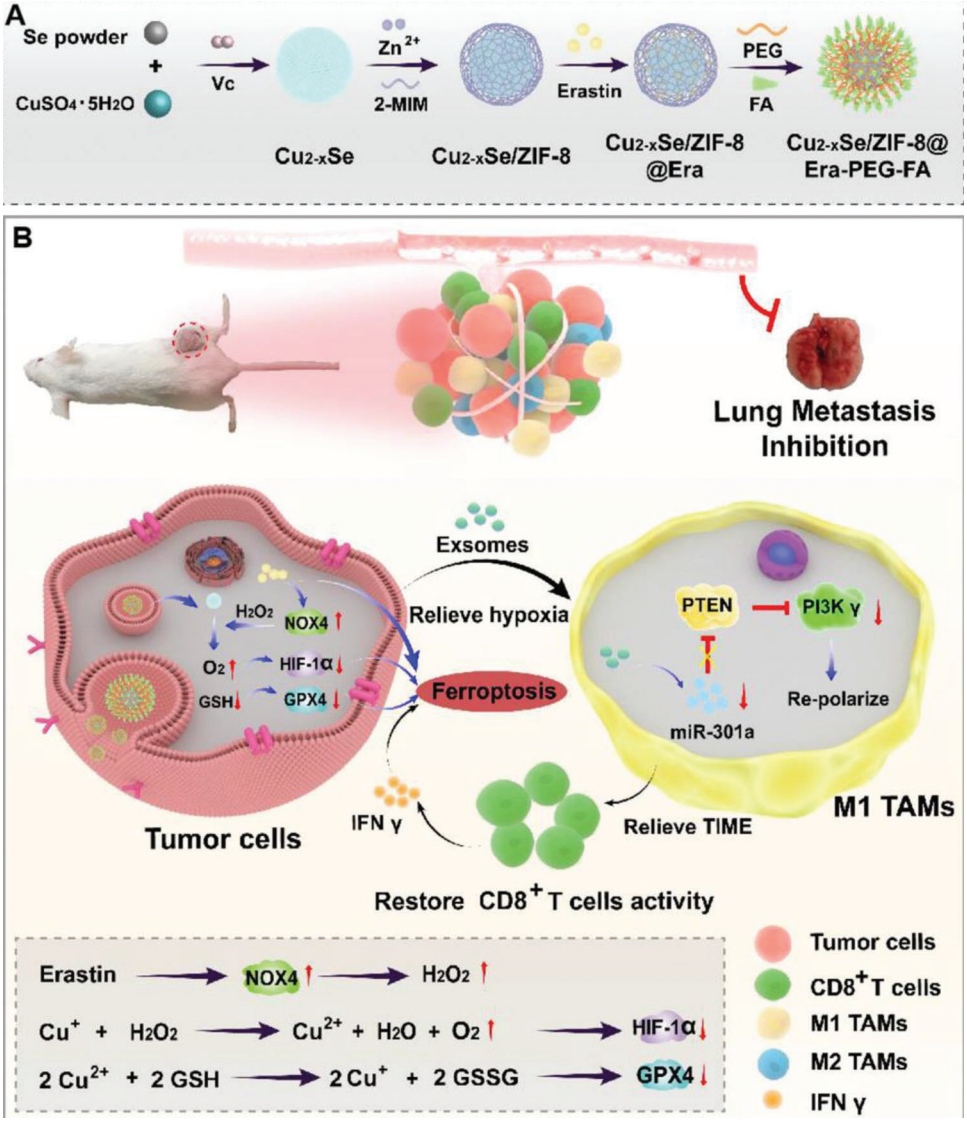


**Figure 15.** Schematic illustration of the multifunctional self-supplying nanoreactor via $O_2$ production and GSH depletion for ferroptosis activation and immunotherapy. A) Synthesis of $Cu_{2-x}Se$/ZIF-8@Era-PEG-FA. B) $Cu_{2-}$xSe/ZIF-8@Era-PEG-FA activate ferroptosis and repolarize TAMs phenotype by reacting with $H_2O_2$ and GSH to produce $O_2$ and consume GSH, relieve immunosuppression, activate an immune response, and inhibit tumor growth. Reproduced with permission.[101] Copyright 2023, American Chemical Society.

FeSHK@B-OVA integrated dual immunostimulants and exhibited prominent tumor inhibition by boosting DC maturation and infiltrating $CD4^+$ helper and $CD8^+$ cytotoxic T cells in tumors (Figure 14B–D). Collectively, those results validated that FeSHK@B-OVA not only effectively inhibited the primary tumor growth and triggered a durable antigen-specific immune response in vivo, but also activated a long-term and powerful immune memory effect to resist tumor recurrence.

Considering the special metabolism, a relatively excess $H_2O_2$ and less GSH existence in tumor cells, and a high concentration of intracellular GSH may participate in the GPX4-regulated ferroptosis pathway. Developing a nanoreactor that simultaneously reacts with $H_2O_2$ and GSH may be a potential strategy to alleviate the tumor hypoxic microenvironment and thereby activate tumor immune responses and ferroptosis. Based on the above conjecture, Zhao et al. proposed a nanoreactor $Cu_{2-x}Se$, which consumed intracellular GSH and produced $O_2$ by conversing copper elements between $Cu^+$ and $Cu^{2+}$. To enhance the ability of nanoreactors to induce ferroptosis, the ZIF-8 coating was modified as the outer layer and loaded with a ferroptosis agonist of erastin (**Figure 15**A), and PEG and folic acid were modified on the surface to form the nanoreactor of $Cu_{2-x}Se$/ZIF-8@Era-PEG-FA.[101] The nanoreactor induced ferroptosis through the following cascades, including the pH-sensitive release of erastin-induced ferroptosis, the depletion of intracellular GSH, increasing intracellular $H_2O_2$, downregulating GPX-4 expression, and up-regulating NOX-4 expression. Moreover, the hypoxic microenvironment was alleviated with the production of $O_2$, and the antagonism of ferroptosis dependent on the expression of HIF-1$\alpha$ and the expression of miR301-a gene was attenuated, which

affected the phenotypic polarization of TAMs and increased the IFN-$\gamma$ cytokines secretion by $CD8^+$ T cells, promoting the ferroptosis (Figure 15B). So, there is no doubt that the combo FT-IT treatments have optimal therapeutic effects and possess great promise in anti-tumor therapy, it should be noted that how to achieve strong ferroptosis-induced ICD in tumors, efficient phagocytosis of dead tumor cells by dendritic cells, robust killing of tumor cells by antigen-specific cytotoxic T cells, and the immune-priming signal pathways of ferroptosis remains challenging and deserves to be deeply investigated.

## 3. Conclusions and Perspectives

In this review, we comprehensively summarize the cancer FT strategies mediated by different biocompatible polymers, which include FT alone and combo FT with other therapies including CT, SDT/PDT, PTT, GT, and IT as well. The main problems that need to be further solved and the perspectives are given as follows.

1) Ferroptosis is an iron-dependent non-apoptotic cell death modality, and the ferrous nanoparticles are typical Fenton reaction reagents to be utilized in cancer nanoplatforms. To boost FT efficacy, one is how to enhance the intracellular delivery and concentration of Fe ions; the other is how to boost the kinetics and efficiency of Fenton reaction by physical triggers (e.g., temperature) or physiological modulation (e.g., pH and $H_2O_2$), and designing other metal-based chemodynamic therapy nanoplatforms with higher Fenton reaction kinetics, such as Cu and Mn ions, etc., is one promising method to improve anticancer efficacy.[102–104]
2) Scientists are committed to the development of "one-for-all" theranostic nanoagents for multiple-imaging-guided combo antitumor therapies while it remains challenging to combine ferroptosis with multiple modalities in one biocompatible nanoplatform, and to regulate simultaneously multiple cell death pathways and amplify synergistic anticancer efficacy via cascade reactions.[105] Notably, the combo ferroptosis treatments such as FT-CT, FT-PTT, FT-GT, FT-IT, and the multimodal integrated ones need further deeper investigation as they are expected to mediate amplified ICD effects and/or immunosuppressive TME to prime potent immunity and long-term immune memory effects for combating intractable and metastatic cancers and the recurrences.[105–107]
3) Some kinds of biocompatible polymers and their degraded products (e.g., PLGA, polypeptides) can be absorbed or completely excreted from the body, however, designing biocompatible polymeric nanomaterials with better tumor/cell targeting, long-circulating time, and fast response to tumor TME or cellular milieu remains to be studied. Meanwhile, the long-term biosafety of nanomaterials still limits clinical applications, and it is wise to optimize the comprehensive properties of ferroptosis nanocarriers without compromising biosafety.[48]
4) At present, biocompatible polymeric ferroptosis nanocarriers and the combo treatments are in a vigorous development stage, and the clinical transition-targeted researches on the ferroptosis and combo treatments should be strived under the multi-discipline cooperation to solve the bedside problems, accelerating them from bench to bedside.

## Acknowledgements

C.M.D thanks for the support by the National Natural Science Foundation of China (22075176) and the Natural Science Foundation of Shanghai (22ZR1429200). M.S.C thanks for the support by Shanghai Pujiang Program (21PJD062), Science and Technology Commission of Shanghai Municipality (21S11900500&22S21903200), and Shanghai Public Health Clinic Center (KYGW202110).

## Conflict of Interest

The authors declare no conflict of interest.

## Keywords

biocompatible polymers, combo therapy, ferroptosis, immunotherapy, nanoplatforms, synergistic effect

Received: May 15, 2023
Revised: June 8, 2023
Published online:

[1] C. Xia, X. Dong, H. Li, M. Cao, D. Sun, S. He, F. Yang, X. Yan, S. Zhang, N. Li, W. Chen, *Chin Med J (Engl)* **2022**, *135*, 584.
[2] W. Y. Zhen, R. R. Weichselbaum, W. B. Lin, *Adv. Mater.* **2023**, *35*, 2206370.
[3] W. Wang, Z. Huang, Y. Huang, X. Pan, C. Wu, *Int. J. Pharm.* **2020**, *589*, 119815.
[4] A. Gulzar, J. T. Xu, C. Wang, F. He, D. Yang, S. L. Gai, P. P. Yang, J. Lin, D. Y. Jin, B. G. Xing, *Nano Today* **2019**, *26*, 16.
[5] S. Kunjachan, J. Ehling, G. Storm, F. Kiessling, T. Lammers, *Chem. Rev.* **2015**, *115*, 10907.
[6] S. G. Alamdari, M. Amini, N. Jalilzadeh, B. Baradaran, R. Mohammadzadeh, A. Mokhtarzadeh, F. Oroojalian, *J. Controlled Release* **2022**, *349*, 269.
[7] B. W. Sun, J. N. B. Rahmat, Y. Zhang, *Biomaterials* **2022**, *291*, 121875.
[8] Z. He, J. Du, Y. Miao, Y. Li, *Adv. Healthcare Mater.* **2023**, e2300234.
[9] S. J. Yu, Z. W. Chen, X. Zeng, X. S. Chen, Z. Gu, *Theranostics* **2019**, *9*, 8026.
[10] S. J. Dixon, K. M. Lemberg, M. R. Lamprecht, R. Skouta, E. M. Zaitsev, C. E. Gleason, D. N. Patel, A. J. Bauer, A. M. Cantley, W. S. Yang, B. Morrison, 3rd, B. R. Stockwell, *Cell* **2012**, *149*, 1060.
[11] C. Liang, X. L. Zhang, M. S. Yang, X. C. Dong, *Adv. Mater.* **2019**, *31*, 1904197.
[12] D. L. Tang, X. Chen, R. Kang, G. Kroemer, *Cell Res.* **2021**, *31*, 107.
[13] B. R. Stockwell, J. P. F. Angeli, H. Bayir, A. I. Bush, M. Conrad, S. J. Dixon, S. Fulda, S. Gascon, S. K. Hatzios, V. E. Kagan, K. Noel, X. J. Jiang, A. Linkermann, M. E. Murphy, M. Overholtzer, A. Oyagi, G. C. Pagnussat, J. Park, Q. Ran, C. S. Rosenfeld, K. Salnikow, D. L. Tang, F. M. Torti, S. V. Torti, S. Toyokuni, K. A. Woerpel, D. D. Zhang, *Cell* **2017**, *171*, 273.
[14] W. Wang, M. Green, J. E. Choi, M. Gijon, P. D. Kennedy, J. K. Johnson, P. Liao, X. Lang, I. Kryczek, A. Sell, H. Xia, J. Zhou, G. Li, J. Li, W. Li, S. Wei, L. Vatan, H. Zhang, W. Szeliga, W. Gu, R. Liu, T. S. Lawrence, C. Lamb, Y. Tanno, M. Cieslik, E. Stone, G. Georgiou, T. A. Chan, A. Chinnaiyan, W. Zou, *Nature* **2019**, *569*, 270.

[15] B. Yu, B. Choi, W. Li, D. H. Kim, *Nat. Commun.* **2020**, *11*, 3637.
[16] X. Wang, Z. Y. Song, S. Q. Wei, G. N. Ji, X. T. Zheng, Z. H. Fu, J. J. Cheng, *Biomaterials* **2021**, *275*, 120913.
[17] Y. T. Xia, J. Z. Zhang, G. Liu, *Nano Today* **2023**, *48*, 101740.
[18] B. Hassannia, P. Vandenabeele, T. Vanden Berghe, *Cancer Cell* **2019**, *35*, 830.
[19] Y. Wang, F. Chen, H. Zhou, L. Huang, J. Ye, X. Liu, W. Sheng, W. Gao, H. Yu, F. Wang, *Small Methods* **2023**, *7*, 2200888.
[20] W. S. Yang, B. R. Stockwell, *Chem. Biol.* **2008**, *15*, 234.
[21] S. V. Torti, F. M. Torti, *Nat. Nanotechnol.* **2019**, *14*, 499.
[22] C. Liang, X. Zhang, M. Yang, X. Dong, *Adv. Mater.* **2019**, *31*, 1904197.
[23] U. Arif, S. Haider, A. Haider, N. Khan, A. A. Alghyamah, N. Jamila, M. I. Khan, W. A. Almasry, I. K. Kang, *Curr. Pharm. Des.* **2019**, *25*, 3608.
[24] T. J. Deming, *Prog. Polym. Sci.* **2007**, *32*, 858.
[25] K. Li, C. J. Liu, X. Z. Zhang, *Adv Drug Deliv Rev* **2020**, *160*, 36.
[26] Y. Zhang, H. Tan, J. D. Daniels, F. Zandkarimi, H. R. Liu, L. M. Brown, K. Uchida, O. A. O'Connor, B. R. Stockwell, *Cell Chem. Biol.* **2019**, *26*, 623.
[27] M. Gao, J. Deng, F. Liu, A. Fan, Y. Wang, H. Wu, D. Ding, D. Kong, Z. Wang, D. Peer, Y. Zhao, *Biomaterials* **2019**, *223*, 119486.
[28] X. Guo, F. Liu, J. Deng, P. Dai, Y. Qin, Z. Li, B. Wang, A. Fan, Z. Wang, Y. Zhao, *ACS Nano* **2020**, *14*, 14715.
[29] S. E. Kim, L. Zhang, K. Ma, M. Riegman, F. Chen, I. Ingold, M. Conrad, M. Z. Turker, M. Gao, X. Jiang, S. Monette, M. Pauliah, M. Gonen, P. Zanzonico, T. Quinn, U. Wiesner, M. S. Bradbury, M. Overholtzer, *Nat. Nanotechnol.* **2016**, *11*, 977.
[30] L. Y. Wang, M. F. Huo, Y. Chen, J. L. Shi, *Biomaterials* **2018**, *163*, 1.
[31] W. Ma, Y. Gao, Z. Ouyang, Y. Fan, H. Yu, M. Zhan, H. Wang, X. Shi, M. Shen, *Sci. China: Chem.* **2022**, *65*, 778.
[32] F. Liu, L. Lin, Y. Zhang, Y. B. Wang, S. Sheng, C. N. Xu, H. Y. Tian, X. S. Chen, *Adv. Mater.* **2019**, *31*, 1902885.
[33] H. Cheng, X. Y. Jiang, R. R. Zheng, S. J. Zuo, L. P. Zhao, G. L. Fan, B. R. Xie, X. Y. Yu, S. Y. Li, X. Z. Zhang, *Biomaterials* **2019**, *195*, 75.
[34] T. Itoh, R. Terazawa, K. Kojima, K. Nakane, T. Deguchi, M. Ando, Y. Tsukamasa, M. Ito, Y. Nozawa, *Free Radical Res.* **2011**, *45*, 1033.
[35] P. Ma, H. Xiao, C. Yu, J. Liu, Z. Cheng, H. Song, X. Zhang, C. Li, J. Wang, Z. Gu, J. Lin, *Nano Lett.* **2017**, *17*, 928.
[36] Z. L. Gao, T. He, P. Y. Zhang, X. Y. Li, Y. L. Zhang, J. Lin, J. C. Hao, P. Huang, J. W. Cui, *ACS Appl. Mater. Interfaces* **2020**, *12*, 20271.
[37] J. L. Nitiss, *Nat. Rev. Cancer* **2009**, *9*, 338.
[38] W. Jiang, X. Y. Luo, L. L. Wei, S. M. Yuan, J. F. Cai, X. Q. Jiang, Y. Hu, *Small* **2021**, *17*, 2102695.
[39] M. Q. Li, Z. H. Tang, S. X. Lv, W. T. Song, H. Hong, X. B. Jing, Y. Y. Zhang, X. S. Chen, *Biomaterials* **2014**, *35*, 3851.
[40] M. Gilleron, X. Marechal, D. Montaigne, J. Franczak, R. Neviere, S. Lancel, *Biochem. Biophys. Res. Commun.* **2009**, *388*, 727.
[41] E. L. G. Samuel, D. C. Marcano, V. Berka, B. R. Bitner, G. Wu, A. Potter, R. H. Fabian, R. G. Pautler, T. A. Kent, A. L. Tsai, J. M. Tour, *Proc. Natl. Acad. Sci. USA* **2015**, *112*, 2343.
[42] Y. Dai, Z. Yang, S. Cheng, Z. Wang, R. Zhang, G. Zhu, Z. Wang, B. C. Yung, R. Tian, O. Jacobson, C. Xu, Q. Ni, J. Song, X. Sun, G. Niu, X. Chen, *Adv. Mater.* **2018**, *30*, 1704877.
[43] X. Chen, R. Kang, G. Kroemer, D. Tang, *Nat. Rev. Clin. Oncol.* **2021**, *18*, 280.
[44] S. S. Lucky, K. C. Soo, Y. Zhang, *Chem. Rev.* **2015**, *115*, 1990.
[45] L. Q. Zhou, C. H. Dong, L. Ding, W. Feng, L. D. Yu, X. W. Cui, Y. Chen, *Nano Today* **2021**, *39*, 101212.
[46] Y. R. Chen, J. Deng, F. Liu, P. P. Dai, Y. An, Z. Wang, Y. J. Zhao, *Adv. Healthcare Mater.* **2019**, *8*, 1900366.
[47] X. Meng, J. Deng, F. Liu, T. Guo, M. Y. Liu, P. P. Dai, A. P. Fan, Z. Wang, Y. J. Zhao, *Nano Lett.* **2019**, *19*, 7866.
[48] B. W. Yang, Y. Chen, J. L. Shi, *Chem. Rev.* **2019**, *119*, 4881.
[49] Q. Chen, X. Ma, L. Xie, W. Chen, Z. Xu, E. Song, X. Zhu, Y. Song, *Nanoscale* **2021**, *13*, 4855.
[50] Z. Zhao, W. Wang, C. Li, Y. Zhang, T. Yu, R. Wu, J. Zhao, Z. Liu, J. Liu, H. Yu, *Adv. Funct. Mater.* **2019**, *29*, 1905013.
[51] D. Li, Y. Yang, D. F. Li, J. Pan, C. C. Chu, G. Liu, *Small* **2021**, *17*, 2101976.
[52] Y. Li, Y. Qin, Y. Q. Shang, Y. R. Li, F. Liu, J. J. Luo, J. D. Zhu, X. L. Guo, Z. Wang, Y. J. Zhao, *Adv. Funct. Mater.* **2022**, *32*, 2112000.
[53] S. Bai, N. L. Yang, X. W. Wang, F. Gong, Z. L. Dong, Y. H. Gong, Z. Liu, L. Cheng, *ACS Nano* **2020**, *14*, 15119.
[54] X. Lin, S. Liu, X. Zhang, R. Zhu, S. Chen, X. Chen, J. Song, H. Yang, *Angew Chem Int Ed Engl* **2020**, *59*, 1682.
[55] Z. Chen, H. Pan, Y. Luo, T. Yin, B. Zhang, J. Liao, M. Wang, X. Tang, G. Huang, G. Deng, M. Zheng, L. Cai, *Small* **2021**, *17*, 2007494.
[56] Y. J. Liu, P. Bhattarai, Z. F. Dai, X. Y. Chen, *Chem. Soc. Rev.* **2019**, *48*, 2053.
[57] N. Xu, X. Zhang, T. Qi, Y. Wu, X. Xie, F. Chen, D. Shao, J. Liao, *MedComm – Biomaterials and Applications* **2022**, *1*, e25.
[58] Y. Zhang, K. Zhang, H. Yang, Y. Hao, J. Zhang, W. Zhao, S. Zhang, S. Ma, C. Mao, *ACS Appl. Mater. Interfaces* **2023**, *15*, 14099.
[59] L. P. Huang, Y. N. Li, Y. N. Du, Y. Y. Zhang, X. X. Wang, Y. Ding, X. L. Yang, F. L. Meng, J. S. Tu, L. Luo, C. M. Sun, *Nat. Commun.* **2019**, *10*, 4871.
[60] M. Chang, Z. Hou, M. Wang, C. Yang, R. Wang, F. Li, D. Liu, T. Peng, C. Li, J. Lin, *Angew Chem Int Ed Engl* **2021**, *60*, 12971.
[61] C. Du, L. Zhou, J. Qian, M. He, Z. G. Zhang, C. Feng, Y. Zhang, R. Zhang, C. M. Dong, *ACS Appl. Mater. Interfaces* **2021**, *13*, 44002.
[62] M. He, C. Du, J. Xia, Z. G. Zhang, C. M. Dong, *Biomacromolecules* **2022**, *23*, 2655.
[63] S. Xie, W. Sun, C. Zhang, B. Dong, J. Yang, M. Hou, L. Xiong, B. Cai, X. Liu, W. Xue, *ACS Nano* **2021**, *15*, 7179.
[64] D. Wu, X. Chen, J. Zhou, Y. Chen, T. Wan, Y. Wang, A. Lin, Y. Ruan, Z. Chen, X. Song, W. Fang, H. Duan, Y. Ping, *Mater. Horiz.* **2020**, *7*, 2929.
[65] Y. Jiang, X. Zhao, J. Huang, J. Li, P. K. Upputuri, H. Sun, X. Han, M. Pramanik, Y. Miao, H. Duan, K. Pu, R. Zhang, *Nat. Commun.* **2020**, *11*, 1857.
[66] X. X. Yao, B. R. Yang, J. Xu, Q. J. He, W. L. Yang, *View-China* **2022**, *3*, 20200185.
[67] L. D. Yu, P. Hu, Y. Chen, *Adv. Mater.* **2018**, *30*, 1801964.
[68] Y. Zhou, S. Fan, L. Feng, X. Huang, X. Chen, *Adv. Mater.* **2021**, *33*, 2104223.
[69] W. Fan, B. C. Yung, X. Chen, *Angew Chem Int Ed Engl* **2018**, *57*, 8383.
[70] Y. Hu, T. Lv, Y. Ma, J. Xu, Y. Zhang, Y. Hou, Z. Huang, Y. Ding, *Nano Lett.* **2019**, *19*, 2731.
[71] X. K. Zhang, S. B. Yang, Q. Wang, W. M. Ye, S. L. Liu, X. Wang, Z. Y. Zhang, L. Y. Cao, X. Q. Jiang, *Chem. Eng. J.* **2021**, *423*, 130083.
[72] H. Yang, F. Jiang, L. Zhang, L. Wang, Y. Luo, N. Li, Y. Guo, Q. Wang, J. Zou, *Biomater. Sci.* **2021**, *9*, 2230.
[73] C. Du, M. Zhou, F. Jia, L. Ruan, H. Lu, J. Zhang, B. Zhu, X. Liu, J. Chen, Z. Chai, Y. Hu, *Biomaterials* **2021**, *269*, 120642.
[74] D. Huang, H. Huang, M. Li, J. Fan, W. Sun, J. Du, S. Long, X. Peng, *Adv. Funct. Mater.* **2022**, *32*, 2208105.
[75] M. He, Y. Song, W. Xu, X. Zhang, C. M. Dong, *Adv. Funct. Mater.* **2023**, 2304216.
[76] Y. Zhou, W. Q. Yu, J. Cao, H. L. Gao, *Biomaterials* **2020**, *255*, 120193.
[77] U. E. Martinez-Outschoorn, M. Peiris-Pages, R. G. Pestell, F. Sotgia, M. P. Lisanti, *Nat. Rev. Clin. Oncol.* **2017**, *14*, 113.
[78] X. X. Yao, P. Yang, Z. K. Jin, Q. Jiang, R. R. Guo, R. H. Xie, Q. J. He, W. L. Yang, *Biomaterials* **2019**, *197*, 268.
[79] L. C. Chen, S. F. Zhou, L. C. Su, J. B. Song, *ACS Nano* **2019**, *13*, 10887.
[80] C. K. Xie, D. Cen, Z. H. Ren, Y. F. Wang, Y. J. Wu, X. Li, G. R. Han, X. J. Cai, *Adv. Sci.* **2020**, *7*, 1903512.

[81] J. Li, L. S. Xie, B. Li, C. Yin, G. H. Wang, W. Sang, W. X. Li, H. Tian, Z. Zhang, X. J. Zhang, Q. L. Fan, Y. L. Dai, *Adv. Mater.* **2021**, *33*, 2008481.
[82] Z. B. Yang, Y. Luo, Y. A. Hu, K. C. Liang, G. He, Q. Chen, Q. G. Wang, H. R. Chen, *Adv. Funct. Mater.* **2021**, *31*, 2007991.
[83] Y. Wang, M. Qian, Y. L. Du, J. L. Zhou, T. T. Huo, W. Guo, M. Akhtar, R. Q. Huang, *Small* **2022**, *18*, 2106168.
[84] K. Wang, Y. Li, X. Wang, Z. Zhang, L. Cao, X. Fan, B. Wan, F. Liu, X. Zhang, Z. He, Y. Zhou, D. Wang, J. Sun, X. Chen, *Nat. Commun.* **2023**, *14*, 2950.
[85] J. C. Del Paggio, *Nat. Rev. Clin. Oncol.* **2018**, *15*, 268.
[86] T. E. Keenan, K. P. Burke, E. M. Van Allen, *Nat. Med.* **2019**, *25*, 389.
[87] S. L. Topalian, J. M. Taube, R. A. Anders, D. M. Pardoll, *Nat. Rev. Cancer* **2016**, *16*, 275.
[88] B. A. Helmink, P. O. Gaudreau, J. A. Wargo, *Immunity* **2018**, *48*, 1077.
[89] J. H. Li, L. J. Huang, H. L. Zhou, Y. M. Shan, F. M. Chen, V. P. Lehto, W. J. Xu, L. Q. Luo, H. J. Yu, *Acta Pharmacol. Sin.* **2022**, *43*, 2749.
[90] Y. Yang, G. H. Nam, G. B. Kim, Y. K. Kim, I. S. Kim, *Adv. Drug Delivery Rev.* **2019**, *151*, 2.
[91] Z. N. L. Chang, A. R. J. Hou, Y. Y. Chen, *Nat. Protoc.* **2020**, *15*, 1507.
[92] Z. Walsh, Y. M. Yang, M. E. Kohler, *Immunol. Rev.* **2019**, *290*, 100.
[93] A. Kalbasi, A. Ribas, *Nat. Rev. Immunol.* **2020**, *20*, 25.
[94] S. Bhandari, R. Kumar, L. Nice, A. Cheema, G. H. Kloecker, *J. Clin. Oncol.* **2020**, *38*, e15148.
[95] H. J. Xu, D. Ye, M. L. Ren, H. Y. Zhang, F. Bi, *Trends Mol. Med.* **2021**, *27*, 856.
[96] C. Yang, M. Wang, M. Chang, M. Yuan, W. Zhang, J. Tan, B. Ding, P. Ma, J. Lin, *J. Am. Chem. Soc.* **2023**, *145*, 7205.
[97] R. Song, T. Li, J. Ye, F. Sun, B. Hou, M. Saeed, J. Gao, Y. Wang, Q. Zhu, Z. Xu, H. Yu, *Adv. Mater.* **2021**, *33*, 2101155.
[98] L. Luo, M. Z. Iqbal, C. Liu, J. Xing, O. U. Akakuru, Q. Fang, Z. Li, Y. Dai, A. Li, Y. Guan, A. Wu, *Biomaterials* **2019**, *223*, 119464.
[99] L. Xie, J. Li, G. Wang, W. Sang, M. Xu, W. Li, J. Yan, B. Li, Z. Zhang, Q. Zhao, Z. Yuan, Q. Fan, Y. Dai, *J. Am. Chem. Soc.* **2022**, *144*, 787.
[100] L. Yu, M. Yu, W. Chen, S. Sun, W. Huang, T. Wang, Z. Peng, Z. Luo, Y. Fang, Y. Li, Y. Deng, M. Wu, W. Tao, *J. Am. Chem. Soc.* **2023**, *145*, 8375.
[101] K. Li, K. Xu, Y. He, Y. L. Yang, M. J. Tan, Y. L. Mao, Y. A. Zou, Q. Feng, Z. Luo, K. Y. Cai, *ACS Nano* **2023**, *17*, 4667.
[102] P. R. Zhao, H. Y. Li, W. B. Bu, *Angew Chem Int Edit* **2023**, *62*, e202210425.
[103] Z. M. Tang, P. R. Zhao, H. Wang, Y. Y. Liu, W. B. Bu, *Chem. Rev.* **2021**, *121*, 1981.
[104] Y. F. Zhou, S. Y. Fan, L. L. Feng, X. L. Huang, X. Y. Chen, *Adv. Mater.* **2021**, *33*, 2104223.
[105] B. R. Stockwell, *Cell* **2022**, *185*, 2401.
[106] X. Chen, R. Kang, G. Kroemer, D. L. Tang, *Nat. Rev. Clin. Oncol.* **2021**, *18*, 280.
[107] W. M. Wang, M. Green, J. E. Choi, M. Gijon, P. D. Kennedy, J. K. Johnson, P. Liao, X. T. Lang, I. Kryczek, A. Sell, H. J. Xia, J. J. Zhou, G. P. Li, J. Li, W. Li, S. Wei, L. Vatan, H. J. Zhang, W. Szeliga, W. Gu, R. Liu, T. S. Lawrence, C. Lamb, Y. Tanno, M. Cieslik, E. Stone, G. Georgiou, T. A. Chan, A. Chinnaiyan, W. P. Zou, *Nature* **2019**, *569*, 270.

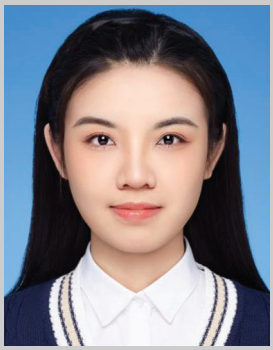

**Meng He** is a Ph.D. candidate in Prof. Dong's group at the School of Chemistry and Chemical Engineering, Shanghai Jiao Tong University, China. Her research interests mainly focus on the synthesis of polypeptide and their biological applications including antitumor ferroptosis and immunotherapy.

**Yuxin Dan** received her Bachelor's degree at Nanjing University of Science and Technology in 2022. She is currently a graduate in Prof. Dong's group at the School of Chemistry and Chemical Engineering, Shanghai Jiao Tong University, China. Her research interests mainly focus on the design and synthesis of polypeptide nanoplatform for drug delivery and cancer immunotherapy.

**Chang-Ming Dong** is a tenured full professor at the School of Chemistry and Chemical Engineering, Shanghai Jiao Tong University, China. He mainly focuses on the design and synthesis of biomedical polymers, drug delivery and anticancer nanomedicines, polymeric hydrogels, and wound dressings.